JOURNAL OF GUIDANCE, CONTROL, AND DYNAMICS
Vol. 43, No. 12, December 2020

Minimum Bounds on Multispacecraft ΔV Optimal Cooperative Rendezvous

Chandrakanth Venigalla* and Daniel J. Scheeres†
University of Colorado Boulder, Boulder, Colorado 80309

https://doi.org/10.2514/1.G004978

Time- and orientation-free ΔV optimal transfers are used to investigate optimal rendezvous orbits for cooperative systems of two and more spacecraft. The problem of finding total ΔV optimal cooperative rendezvous orbits is formulated and solved as a nonlinear programming problem using analytic expressions for optimal orbit transfer ΔV costs. Each spacecraft has propulsive abilities, and optimal rendezvous orbits are found for planar (match semimajor axis and eccentricity) and three-dimensional (match semimajor axis, eccentricity, and inclination) scenarios. The ΔV costs found for this type of rendezvous are lower-bound costs for finite-time full rendezvous where all spacecraft would have matching sets of all six orbit elements. This lower-bound ΔV cost, which is realizable for full rendezvous given infinite time and secular J_2 perturbations, is shown to be also realizable for finite-time full rendezvous if certain initial conditions can be met. Finally, application of the cooperative rendezvous problem to constellation deployment is briefly discussed.

Nomenclature

a	=	semimajor axis, km
e	=	eccentricity
F	=	implicit function used to solve for η^*
i	=	inclination, deg
J^*	=	optimal two-impulse cost for one spacecraft to transfer from one orbit to another, km/s
J_{total}	=	sum of J^* values for all spacecraft to transfer to a single final orbit, km/s
M	=	mean anomaly, rad
N	=	number of spacecraft
n	=	mean motion, rad/s
n_q	=	number of discrete values of i_f for which to calculate J_{total}
n_Q	=	number of discrete values of Q_f for which to calculate J_{total}
n_i	=	number of discrete values of q_f for which to calculate J_{total}
Q	=	radius of apoapsis, km
q	=	radius of periapsis, km
r_c	=	radius of the central body, km
T	=	orbital period, s
t_{tr}	=	time for spacecraft to transfer from initial to final orbit, s
v_f	=	spacecraft speed after the second Hohmann transfer maneuver, km/s
v_0	=	spacecraft speed before first Hohmann transfer maneuver, km/s
v_{1t}	=	spacecraft speed after the first Hohmann transfer maneuver, km/s
v_{2t}	=	spacecraft speed before the second Hohmann transfer maneuver, km/s
$\Delta V'_{\text{total}}$	=	planar Hohmann transfer cost, km/s
ΔV_1	=	first-maneuver ΔV for nonplanar two-impulse transfer, km/s
ΔV_2	=	second-maneuver ΔV for nonplanar two-impulse transfer, km/s
η	=	fraction of total inclination change performed at first maneuver in two-impulse three-dimensional sequence
μ	=	gravitational parameter, km^3/s^2
Ω	=	right ascension of the ascending node, deg
ω	=	argument of periapsis, deg

Subscripts

f	=	orbital element of final orbit (posttransfer)
tr	=	parameter corresponding to the transfer orbit
0	=	orbital element of initial orbit (pretransfer)

I. Introduction

THERE is a growing interest in spacecraft mission architectures that take advantage of two or more spacecraft. These missions include spacecraft swarms, formation flying, and constellation missions where multiple spacecraft have propulsive abilities. These types of missions allow for increased robustness and can provide capabilities that are not possible with single-spacecraft mission architectures. However, tools available to mission planners for large numbers of spacecraft are limited, making mission design for these systems more complicated. It is difficult to understand and take advantage of the full capabilities of multispacecraft systems without the development of new optimization tools. Decades of work on single-spacecraft trajectory design and analysis has given practitioners crucial intuition for solving those types of problems. Such intuition for multispacecraft problems is relatively lacking. Although there has certainly been a significant amount of work completed to explore questions of how to best use and control systems of multiple spacecraft, there is much more to learn about how these systems fundamentally behave. A great deal of related past work can be found in the comprehensive survey papers of Scharf et al. [1,2] that briefly describe and cite previous work done on spacecraft formation-flying guidance and control. Another slightly more recent work is the textbook by Alfriend et al. [3], which aims to describe in some detail the various aspects of Earth-orbiting formation flying (it does not include discussions of deep-space or libration-point formation flying). In the interest of furthering the community's fundamental understanding of multispacecraft systems, we investigate the application of time- and orientation-free spacecraft orbit transfers to find lower bounds on the cost for ΔV optimal rendezvous orbits in multispacecraft systems.

Orbital time- and orientation-free transfers are those in which the transfer time is not specified or restricted, and the final argument of periapsis is also unspecified [4]. Perhaps the most familiar time- and orientation-free transfer in astrodynamics is the Hohmann transfer [5],

Received 26 November 2019; revision received 29 May 2020; accepted for publication 6 June 2020; published online 18 August 2020.

*Ph.D. Student, Aerospace Engineering Sciences. Student Member AIAA.
†A. Richard Seebass Endowed Chair Professor, Aerospace Engineering Sciences. Fellow AIAA.

the ΔV optimal two-impulse transfer between circular orbits. Many early investigations into orbit transfers were similarly based on time- and orientation-free transfers as well (see Gobetz and Doll [4] for a survey of early work). This early work on elementary optimal orbit transfer theory set bounds on the best case performance realizable in a number of different scenarios, and set the foundation for future work on the optimization of orbit transfers for more constrained problems. More recent work by Holzinger et al. [6] has also used time- and orientation-free transfers. Their work specifically focused on applying time-free ΔV optimal orbit transfers in semimajor axis (a), eccentricity (e), and inclination (i) space without specifying final orbit argument of periapsis (ω), right ascension of the ascending node (RAAN, Ω), or mean anomaly (M). Those constraints and optimal control theory were used to determine reachable sets of orbits for different amounts of available ΔV for a spacecraft at a given orbit. Reachable sets were found using level set methods to solve the Hamilton–Jacobi–Bellman partial differential equation.

Spacecraft rendezvous has been explored in a wide variety of scenarios. However, the specific case of cooperative rendezvous with two or more active spacecraft is not explored as frequently in the literature. Spacecraft rendezvous is usually treated in cases of only two spacecraft, most often with an inert or nonmaneuvering target (e.g., space station, target orbit). Here, we generally define "cooperative rendezvous" to be rendezvous where both spacecraft actively maneuver, and the rendezvous orbit is not necessarily constrained to be the initial orbit of one of the constituent spacecraft. Two-spacecraft, fuel-optimal cooperative rendezvous has been explored with an optimal control approach by Prussing for finite-thrust rendezvous to match unconstrained final position and velocity [7] as well as for an impulsive terminal maneuver to match velocities of two spacecraft with already matching positions [8,9]. Coverstone and Prussing have also investigated power-limited rendezvous between circular orbits using linearized [10] and nonlinear [11] two-body dynamics, also with an optimal control approach. Dutta and Tsiotras explored analytic solutions to planar cooperative rendezvous scenarios given fixed-time transfers, circular initial orbits, and circular rendezvous orbits [12]. Bevilacqua and Romano explored the use of differential drag with a control law for cooperative rendezvous of multiple spacecraft ($N > 2$) at a target spacecraft using linearized dynamics [13]. Thakur et al. [14] developed a decentralized, stable control scheme that is used to bring a swarm of low-thrust spacecraft ($N > 2$) into the same orbit at different anomaly angles. A decentralized scheme is used to allow each spacecraft to decide its own control while only knowing the states of neighboring spacecraft. In that work a final orbit semimajor axis and eccentricity are prescribed, whereas the final orbit plane is decided on by a consensus protocol that is not optimizing factors such as time or fuel.

The present work considers the question of where the ΔV optimal meeting point is for an arbitrary number of actively maneuvering spacecraft. The rendezvous orbit is unconstrained in order to enable the freedom to choose a total ΔV optimal rendezvous point or an orbit that optimizes some other ΔV-based criteria. If ΔV savings can be realized by careful selection of an unconstrained rendezvous orbit, this may enable mission designers to more efficiently design a multispacecraft system and could perhaps enable new architectures, especially when a design is ΔV limited. Answering this question is also key to trajectory design for scenarios where there is no obvious rendezvous point such as the orbit of a space station. In scenarios without an obvious or highly constrained rendezvous orbit, the location of the final rendezvous orbit itself may be less important than minimizing the cost of rendezvous. This is especially true when the total available ΔV is limited, such as in small satellite missions. Examples of such scenarios include on-orbit construction and on-orbit placement of supply depots (e.g., placing a supply depot or servicing spacecraft at the ΔV optimal rendezvous location). The question considered here is a similar problem to the scenario addressed by Thakur et al. [14], but we instead focus on finding the semimajor axis, eccentricity, and inclination of ΔV optimal rendezvous orbits in a centralized scenario where a central actor knows all spacecraft states and can direct the actions of all spacecraft.

In Sec. II we first discuss the assumptions made, and then describe how to calculate ΔV optimal orbit transfer costs under those assumptions. Notably, the orbit transfer costs found with the method of Sec. II only account for orbit transfers in a, e, and i space without regard for costs to achieve a certain ω, Ω, and M. However, desired ω, Ω, and M values can be achieved at no ΔV cost given infinite time and secular perturbations due to J_2. Using that method, in Sec. III we formulate the cooperative ΔV optimal rendezvous orbit problem as a nonlinear programming problem (NLP) and discuss methods of solving it. The resulting solution for ΔV optimal rendezvous presents the optimal cost for full rendezvous (all six orbit elements match for all spacecraft attempting rendezvous) if an infinite amount of time is available to complete all transfers. Orbit elements a, e, and i of the rendezvous orbit are found with the solution method developed here, whereas the other orbit elements do not impact the time-free cost. Unless otherwise specified, the term "rendezvous" in this paper will refer to this time-free rendezvous where ΔV is only expended to make each spacecraft have a matching set of a, e, and i, and other orbit elements are allowed to naturally match with no additional ΔV cost by using secular J_2 perturbations. The time-free ΔV cost found for all spacecraft to meet at the optimal rendezvous orbit is a lower bound for the ΔV cost for finite-time full rendezvous where the total transfer time cannot be infinite and for situations where there is no J_2 perturbation to cause propellant free changes in ω, Ω, and M. Section IV explores planar scenarios (a, e) and three-dimensional scenarios (a, e, i) within this framework of finding bounding time-free ΔV costs for cooperative rendezvous. In both scenarios, instances with $N = 2$ spacecraft as well as $N > 2$ spacecraft are addressed.

In Sec. V.A, we use an example to demonstrate that the optimal time-free ΔV cost for rendezvous found with the method of Sec. III can also be equal to the ΔV cost of finite-time full rendezvous if certain initial conditions are able to be selected. The same maneuvers found in the time-free case can also be used to achieve the time-free ΔV cost while achieving full rendezvous in finite time. Finally, because spacecraft deployment is similar to spacecraft rendezvous in reverse in this work, Sec. V.B includes a discussion of applying the ΔV optimal rendezvous solution to constellation deployment scenarios. The ΔV optimal rendezvous orbit for a set of spacecraft already in their final orbits represents the initial or deployment orbit that has the lowest total ΔV cost for all spacecraft to transfer to their final orbits.

II. Time- and Orientation-Free Optimal Transfers in Three Dimensions

The original motivation of this work was to apply the reachable set methods of Holzinger et al. [6] to multispacecraft scenarios. Although doing so is possible [15], we found that the level set methods used to calculate the reachable sets were in practice cumbersome to work with; calculating sets at high accuracies took a considerable amount of computation time and only gave results at discrete locations. For multispacecraft scenarios, such limitations make analysis especially difficult because the points of interest are those where the reachable sets of different spacecraft intersect. In this work we instead focus on using known optimal transfer sequences between orbits to address multispacecraft scenarios. Calculating the optimal ΔV from the fixed initial condition to a final orbit is equivalent to solving for a single point on a full reachable set surface. This has the advantage of allowing the exact, analytic calculation of transfer ΔV costs between orbits in a much faster manner than solving for a full reachable set of orbits.

In this work we make similar assumptions to those made in the work of Holzinger et al. [6]. Maneuvers are assumed to be impulsive, there is no constraint on transfer time, and the final angles ω, Ω, and M are not specified for the final orbit when transferring from one orbit to another. For planar transfers, the final orbit inclination is also unspecified. Most of this work assumes Keplerian dynamics, whereas Keplerian dynamics with secular effects from J_2 are used in Sec. V.A. Note that there is no secular effect from J_2 on a, e, and i. Orbit transfers here go from an initial orbit $[\,a_i \quad e_i \quad i_0\,]$ to a final orbit $[\,a_f \quad e_f \quad i_f\,]$. For planar results, orbit transfers go from an initial orbit $[\,a_i \quad e_i\,]$ to a final orbit $[\,a_f \quad e_f\,]$. Throughout this work, the planar orbit shape $[\,a \quad e\,]$ will be treated as equivalent to an orbit parameterization $[\,q \quad Q\,]$ with periapsis radius $q = a(1 - e)$ and apoapsis radius $Q = a(1 + e)$. ΔV optimal transfers in the three-dimensional and planar cases will form the basis of the rendezvous analyses.

Although the time- and orientation-free transfers used here do not specifically target ω, Ω, and M, perturbations from the J_2 spherical harmonic term will cause a secular drift in these parameters (the two-body drift rate in mean anomaly is modified by the J_2 perturbation). Thus, given a gravity field with a J_2 perturbation and no restriction on transfer time, any desired ω, Ω, and M can be achieved at a single instant in time at no ΔV cost by waiting until the secular perturbations cause the orbit to precess into the proper orientation and anomaly angle. Note that for this to be true, no two angular rates ($(d\bar{\omega}/dt)$, $(d\bar{\Omega}/dt)$, $(d\bar{M}/dt)$; the bar denotes orbit-averaged quantities) can be equal to one another or commensurate with one another. This is usually the case in Earth orbit, but the amount of time necessary to reach the desired values of ω, Ω, and M can potentially be infinite or impractically large for a given set of initial conditions and desired final conditions. If the initial values of ω, Ω, and M can be selected, any final values of those orbit elements can be achieved at no cost by selecting initial values such that they drift into the final desired values over the known transfer time (see Sec. V.A for details). Holzinger et al. [6] make a similar case about zero ΔV cost changes to ω and Ω when using optimal control theory to generate reachable sets of orbits in a–e–i space. Without considering J_2 effects, the results will still give a lower bound on the ΔV cost for a transfer that does have additional constraints on ω, Ω, and/or M.

We also limit the number of impulses to two, in part to simplify the analysis. Although it has been shown that for the orientation-free ellipse-to-ellipse transfer (equivalent to the case where both the initial and final ellipse have the same argument of periapsis) there are three-impulse transfers through infinity that can cost less ΔV than two-impulse transfers in some cases [4,16], such transfers are quite extreme. Transfers through infinity use a parabolic trajectory to reach a distance infinitely far from the central body, at which point one or more maneuvers are performed (e.g., a biparabolic transfer). Reachable sets generated with the two-impulse transfers used here look qualitatively similar to those generated by Holzinger et al., though quantitative comparisons are difficult due to the accuracies of the nonanalytically generated reachable sets. We also show in Sec. IV.A that we find the same ΔV optimal rendezvous orbits as in the case where the nonanalytically generated reachable sets are used.

A. Planar Orbit Transfers

The planar transfer case is that of finding an optimal transfer between two coplanar, elliptical orbits. The ΔV optimal transfer sequence for this scenario is well understood and has been proven in a number of different ways; the work of Mease and Rao [17] is one such explanation of the optimal maneuvers. To summarize, the optimal transfer pathways are along lines of constant periapsis and apoapsis, so throughout this work orbits are parameterized with radius of periapsis (q) and radius of apoapsis (Q).

The optimal transfer sequence from an initial orbit Y to several possible final orbits is shown in Fig. 1. For a given initial orbit, the optimal transfer sequence is dictated by the target orbit's apoapsis radius. If the target orbit has a larger apoapsis radius than the initial orbit, then the optimal transfer sequence is to first change the apoapsis radius to match the target apoapsis, and then change the periapsis radius to match the target. This is equivalent to following the path from orbit Y to orbit A or B in Fig. 1. If the target orbit has a smaller apoapsis radius, then the optimal transfer sequence is to first change the periapsis radius to match the target periapsis, and then change the apoapsis radius to match the target. This is equivalent to following the path from orbit Y to orbit C or D in Fig. 1.

For two-impulse transfers, these optimal sequences are accomplished with a combination of two tangential maneuvers at periapsis and apoapsis. For example, to move from orbit Y to orbit A, the spacecraft will first apply a ΔV tangentially at periapsis to raise apoapsis to match A, and then it will apply a ΔV tangentially at apoapsis to lower periapsis to match A. To achieve the optimal ΔV cost, however, the periapsis and apoapsis maneuvers need not occur all in one impulse. That is, the spacecraft could split the apoapsis raise maneuver into multiple maneuvers happening at successive passes of periapsis, and then after finally achieving the desired final apoapsis radius it could split the periapsis changing maneuver into multiple impulses all occurring at different passes of apoapsis. Splitting a periapsis or apoapsis change into multiple impulses will cost the same amount of ΔV as a single maneuver because each submaneuver can be linearly combined to get the same cost. Importantly, all apoapsis change maneuvers must be completed before changing periapsis when the target has a larger apoapsis, or vice versa when the target has a smaller apoapsis. These maneuvers are also consistent with the allowed ΔV optimal maneuvers in Holzinger et al.'s work on generating reachable sets [6].

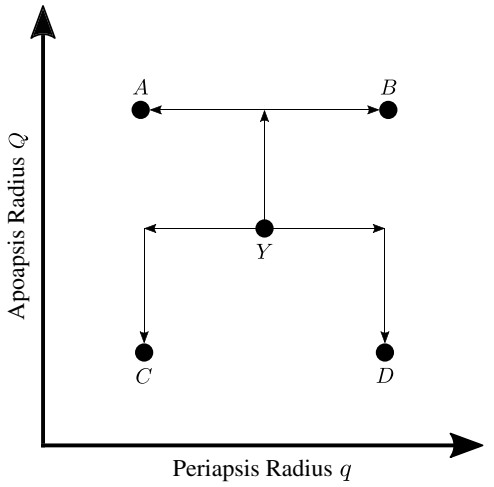

Fig. 1 Optimal transfer pathways.

Note the symmetry present here; the optimal transfer sequence to move to a target orbit is simply reversed if moving from the target orbit to the initial orbit. Degenerate cases where the target orbit has the same radius of periapsis or apoapsis as the initial orbit simply result in one of the two impulsive maneuvers having a magnitude of 0.

Given that the optimal transfer pathways are known, an expression for the optimal ΔV from some initial orbit to any final orbit is

$$\Delta V'_{\text{total}} = \Delta V'_1 + \Delta V'_2 \tag{1}$$

where

$$\Delta V'_1 = |v_{1t} - v_0| \tag{2}$$

$$\Delta V'_2 = |v_f - v_{2t}| \tag{3}$$

and subscript "t" is for the transfer orbit. v_0 is the velocity on the initial orbit immediately before the first impulse, and v_f is the velocity on the final orbit immediately after the second impulse. The optimal two-impulse transfer sequence and ΔV cost relies on the values of the initial and final radius of apoapsis Q_0 and Q_f, where q_0 and q_f are the initial and final periapsis radii. For $Q_f > Q_0$,

$$v_0 = \sqrt{\frac{2\mu}{q_0 + Q_0}\frac{Q_0}{q_0}} \tag{4}$$

$$v_{1t} = \sqrt{\frac{2\mu}{q_0 + Q_f}\frac{Q_f}{q_0}} \tag{5}$$

$$v_{2t} = \sqrt{\frac{2\mu}{q_0 + Q_f}\frac{q_0}{Q_f}} \tag{6}$$

$$v_f = \sqrt{\frac{2\mu}{q_f + Q_f}\frac{q_f}{Q_f}} \tag{7}$$

For $Q_f \leq Q_0$,

$$v_0 = \sqrt{\frac{2\mu}{q_0 + Q_0}\frac{q_0}{Q_0}} \tag{8}$$

$$v_{1t} = \sqrt{\frac{2\mu}{q_f + Q_0}\frac{q_f}{Q_0}} \tag{9}$$

$$v_{2t} = \sqrt{\frac{2\mu}{q_f + Q_0}\frac{Q_0}{q_f}} \tag{10}$$

$$v_f = \sqrt{\frac{2\mu}{q_f + Q_f}\frac{Q_f}{q_f}} \tag{11}$$

Equations (2) and (3) can be rewritten without absolute value operators with knowledge of the initial and final states. This is easier to see if Eqs. (4–11) are rewritten in a different form. For example, Eq. (4) can be rewritten as

$$v_0 = \sqrt{2\mu\left(\frac{1}{q_0} - \frac{1}{q_0 + Q_0}\right)} \tag{12}$$

which enables clearer magnitude comparisons with other velocities. One important note is that the optimal ΔV cost will not have continuous derivatives as the final orbit parameters q_f and Q_f are changed. Discontinuities in partial derivatives of Eqs. (2) and (3) with respect to the final orbit ($\partial/\partial q_f$, $\partial/\partial Q_f$) arise for two reasons. First, because the optimal transfer sequence changes depending on whether Q_f is greater than or less than Q_0, the derivatives will be discontinuous across the line where $Q_0 = Q_f$. Second, the derivatives of Eqs. (2) and (3) are discontinuous because of the absolute value operator. Even if the expressions are rewritten to be positive based on known values of q_0, Q_0, q_f, and Q_f, the derivative is only continuous for limited regions where the difference in certain values has a constant sign.

B. Three-Dimensional Transfers

The ΔV cost of an optimal two-impulse transfer can also be found for the case where an inclination change is included with the orbit shape change. Chobotov [18] has given the optimal two-impulse transfer to perform the orbit transfer of interest here. This transfer has been called a "Mod-2 Hohmann" transfer as well as a "dogleg" maneuver, and although it has not been rigorously proven in [18] to be the optimal transfer policy for this case, it is the best known transfer for minimizing ΔV. This optimal transfer entails using the same two-impulse sequence as discussed for the planar transfer, but both impulses occur at a node and have added out-of-plane components that sum to give the total inclination change needed. Thus, the ΔV cost of each impulse can be calculated by applying the law of cosines to a velocity triangle. This velocity triangle has initial and final velocities defined by the ellipse-to-ellipse Hohmann transfer discussed above, and the angle between the initial and final velocities is some fraction of the total inclination change. Given that the angle between the two velocity vectors is some direct fraction of the total inclination change, the maneuvers are assumed to occur at the ascending or descending node of the orbit. The two velocity triangles used to calculate the cost of each impulse are shown in Fig. 2. Additional information and analysis on the "Mod-2 Hohmann" transfer can be found in previous work [19,20]. These maneuvers are consistent with Holzinger et al.'s enumeration of valid candidates for optimal impulsive maneuvers (see Table 1 in [6]), but when selecting a minimal set of optimal maneuvers they discard inclination changes at periapsis because those maneuvers do not locally maximize the Hamiltonian. Here, we use inclination changes at periapsis because we are selecting each maneuver with the knowledge of what the next maneuver and inclination change will be. In contrast, in Holzinger et al.'s approach there is no a priori knowledge of what future maneuvers will be, so the locally optimal maneuver is selected to maximize the growth of the reachable set.

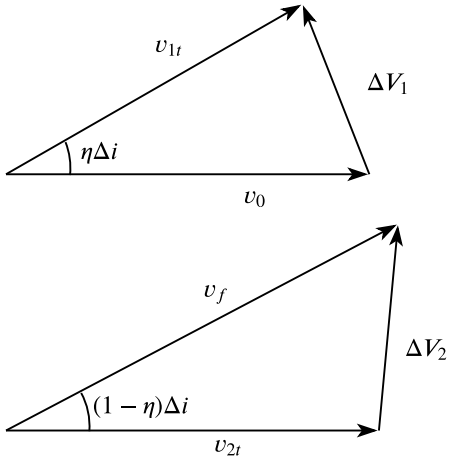

Fig. 2 Velocity triangles used to calculate ΔV_1 and ΔV_2.

Table 1 Constants used for calculations

Constant	Value
Radius of Earth (r_c)	6378 km
J_2	0.0010826269
Gravitational parameter of Earth (μ)	3.986004415×10^5 km^3/s^2

The general expression for the optimal ΔV cost to transfer from one elliptical orbit to another elliptical orbit in a different plane using a two-impulse sequence is

$$J(q_0, Q_0, i_0, q_f, Q_f, i_f) = \Delta V_{\text{total}} = \Delta V_1 + \Delta V_2$$
$$= \sqrt{v_{1t}^2 + v_0^2 - 2v_{1t}v_0\cos(\eta\Delta i)} + \sqrt{v_f^2 + v_{2t}^2 - 2v_{2t}v_f\cos((1-\eta)\Delta i)} \tag{13}$$

This equation combines the planar and out-of-plane maneuvers using the law of cosines. Fractional inclination changes at each of the two impulses are dictated by the parameter η, which is defined in the range $0 \leq \eta \leq 1$. Also note that

$$\Delta i = |i_f - i_0| \tag{14}$$

The η^* that minimizes ΔV_{total} can be found by taking the partial derivative of Eq. (13) with respect to η and equating it to 0. The result,

$$F = \frac{\partial \Delta V_{\text{total}}}{\partial \eta} = \frac{\Delta i v_0 v_{1t}\sin(\eta^*\Delta i)}{\Delta V_1} - \frac{\Delta i v_f v_{2t}\sin((1-\eta^*)\Delta i)}{\Delta V_2} = 0 \tag{15}$$

cannot be explicitly solved for η. The implicit function can, however, be solved using a variety of techniques; in this work a bisection method is used to find the correct value for each individual transfer. The bisection method has the benefit of being able to constrain the solution to within the correct bounds for η, which are $0 \leq \eta \leq 1$. Potentially faster methods such as a Newton–Raphson solver are not as robust and can converge to solutions that exist outside of the allowed domain of η. In degenerate cases where $v_0 = v_{1t}$ and/or $v_f = v_{2t}$, Eq. (15) can be simplified to avoid undefined behavior.

Partial derivatives of the cost in Eq. (13) will be important for a number of reasons discussed throughout this work. Details of the calculations, however, are included in the Appendix.

III. Calculation of Time-Free ΔV Costs for Rendezvous

The analytic expressions for quick computation of optimal transfer costs from one orbit to another can be used to find total ΔV optimal rendezvous orbits. However, an important caveat is that for the multispacecraft case, minimizing ΔV is no longer equivalent to minimizing propellant mass, because in general multiple spacecraft do not have equivalent masses and characteristic velocities. Thus, the ΔV optimal results here are closest to mass optimal results when all spacecraft have the same mass and I_{sp}, and are less linked to mass optimal results as the spacecraft masses and I_{sp} values diverge. Rendezvous here is defined as having all spacecraft attain the same $[a_f \quad e_f \quad i_f]$, or the same $[a_f \quad e_f]$ for the planar case, again because we are finding time-free optimal ΔV costs for rendezvous. For time-free rendezvous, the angles ω, Ω, and M are assumed to match for all spacecraft at some time in the future given secular precession of these angles due to J_2. This comes at no additional ΔV cost, so the cost found here is the optimal cost for time-free rendezvous. The single minimum ΔV rendezvous orbit for a system of N spacecraft gives the optimal cost

$$J^*_{\text{total}} = \min_{q_f, Q_f, i_f} J_{\text{total}} \tag{16}$$

where

$$J_{\text{total}}(q_f, Q_f, i_f) = \sum_{j=1}^{N} J_j \tag{17}$$

$$J_j = J(q_{0,j}, Q_{0,j}, i_{0,j}, q_f, Q_f, i_f) \tag{18}$$

and J is defined by Eq. (13). J_{total} is simply the sum of the optimal costs for each spacecraft to transfer to a specific final orbit. The problem of minimizing Eq. (16) is a variant of the well-known Weber problem. The Weber problem, as stated by Drezner and Hamacher [21], is the problem of finding a point "which minimizes the sum of weighted Euclidean distances from itself to n fixed points." In the spacecraft rendezvous case as formulated here, the point to be found in the Weber problem is the rendezvous orbit, and the weighted distances are the ΔV costs for each spacecraft to transfer to the rendezvous orbit. Although there is a long history of work done on the Weber problem, including some solutions to simpler instances of the problem, none of the past methods of solution for the Weber problem appear to give more insight than the techniques discussed below.

The problem of minimizing Eq. (16) by choosing q_f, Q_f, i_f is more generally a parameter optimization/nonlinear programming problem. There are a wide number of well-developed techniques that can be used to solve this class of problem, including gradient-based methods, genetic algorithms, and grid searches.

Caution must be used when applying gradient-based methods to solving this problem. In addition to the usual concern about only finding local minima, this problem specifically has several boundaries across which the cost function derivatives are not continuous. As discussed in the Appendix, the boundaries occur because the optimal orbit transfer sequence can change depending on the relative values of the initial and final orbits. Thus, as the values of q_f, Q_f, i_f are changed across certain boundaries, the optimal transfer sequence to calculate $J(q_{0,j}, Q_{0,j}, i_{0,j}, q_f, Q_f, i_f)$ will also change, leading to discontinuous derivatives of $J_{\text{total}}(q_f, Q_f, i_f)$. Consequently, gradient-based searches would need to be performed separately in different areas, bounded in regions where the derivatives are continuous. Further, as the number of spacecraft in the system increases, the number of these separate regions with differing cost function derivatives also increases. However, gradient-based methods are useful for local optimization, and the partial derivatives provided in the Appendix can be applied to the larger problem of minimizing Eq. (16).

In much of this work, a grid search is instead used to explore the structure of solutions to this problem for differing initial conditions. The grid search approach gives insight into the structure of the solutions to the scenarios explored here, whereas other approaches result in single optima without necessarily giving an understanding of the overall solution space. The grid search solution, however, comes at the expense of computation time. Minima found using a grid search can subsequently be refined using an NLP solver such as Interior Point OPTimizer (IPOPT).

To perform the grid search, Eq. (13) is used to calculate the optimal two-impulse ΔV costs for a spacecraft with given initial conditions $(q_{0,j}, Q_{0,j}, i_{0,j})$ to transfer to a discrete grid of final orbits in q–Q–i space. For a single spacecraft, this grid allows the computation of the reachable set of orbits for a given amount of available ΔV. For systems of multiple spacecraft, grids from each spacecraft can be summed together to give the cost for all spacecraft to meet at any given orbit in the grid. Exploring this summed grid to find minimum total ΔV rendezvous orbits is equivalent to performing a grid search for the optimal q_f, Q_f, i_f.

The grid search method used here is summarized in Algorithm 1.

Algorithm 1: J^*_{total} computation algorithm

Result: Optimal cost J^*_{total}
for $k = 1, 2, \ldots, n_q$ **do**
  for $l = 1, 2, \ldots, n_Q$ **do**
    for $m = 1, 2, \ldots, n_i$ **do**
      $J_{\text{total}}(q_{f,k}, Q_{f,l}, i_{f,m}) \leftarrow 0$;
      for $j = 1, 2, \ldots, N$ **do**
        $\eta^* \leftarrow$ Eq. (15) solution;
        $J_j \leftarrow J^*(q_{0,j}, Q_{0,j}, i_{0,j}, q_{f,k}, Q_{f,l}, i_{f,m}, \eta^*)$ (Eq. (13));
        $J_{\text{total}}(q_{f,k}, Q_{f,l}, i_{f,m}) \leftarrow J_{\text{total}}(q_{f,k}, Q_{f,l}, i_{f,m}) + J_j$;
      end
  End
  End
End
$J^*_{\text{total}} \leftarrow \min[J_{\text{total}}(q_{f,1:n_q}, Q_{f,1:n_Q}, i_{f,1:n_i})]$

For a system of N spacecraft, the algorithm finds the minimum rendezvous orbit cost J^*_{total} using a grid of n_q values of q_f, n_Q values of Q_f, and n_i values of i_f.

Computing dense grids is relatively fast because calculating the ΔV optimal transfer costs relies on a mostly analytic expression. The root-finding algorithm necessary to find an optimal value of η does, however, make the computation slower. Still, computing a grid of 1 million costs J_{total} for a system of four spacecraft takes only 7 minutes on a laptop with a four-core processor. Further, this method lends itself to parallelization on larger-scale computing platforms (e.g., supercomputers) because each computation of Eq. (13) is independent.

Alternative, derivative-free solution methods (genetic algorithms and particle swarm optimization) have given very similar results as the grid search method, but with a vastly improved runtime. However, without a grid search solution as a point of comparison, the level of confidence in the solution may or may not be high enough for a given scenario or use case. For operational purposes, the problem may best be solved with a hybrid evolutionary algorithm and NLP solver method.

IV. Time-Free ΔV Optimal Rendezvous Solutions

A. Two-Spacecraft, Planar Rendezvous

In the planar, two-spacecraft case, there is no single, unique ΔV optimal rendezvous orbit. Rather, there is a continuous set of optimal rendezvous orbits that occurs along the transfer path between both spacecraft. The transfer path is dictated by the relative orbital positions of the two spacecraft (see Fig. 1), and any point along that path may be selected as the rendezvous orbit to achieve a minimum total ΔV rendezvous. Because the total ΔV for rendezvous is the same at any point along this path, the path is called the "invariant curve." A free parameter here is the relative ΔV expended by each spacecraft to reach the rendezvous orbit. Different rendezvous orbits along the

invariant curve will require different relative ΔV expenditures by each spacecraft. This result arises because transfers along the invariant curve can be split into an infinite number of impulses, as discussed in Sec. II.A. Thus, both spacecraft can incrementally move along the optimal transfer pathways (while maneuvering only at periapsis or apoapsis) until they meet without making the overall transfer suboptimal.

This result can be seen through example grid search results for two-spacecraft planar rendezvous in low Earth orbit (LEO) in Figs. 3 and 4 ($\mu = 3.986004415 \times 10^5$ km^3/s^2). Because the grid search is parameterized in radius of periapsis and radius of apoapsis space, the invariant curve can clearly be seen as a set of discrete points all with minimum total ΔV for rendezvous. The minimum total ΔV rendezvous orbits, shown with green circles, match exactly the orbits that are along the optimal transfer pathway between the two spacecraft initial orbits. Figure 4 shows a simplified view with total rendezvous ΔV contour lines, and red squares show the initial spacecraft orbits. Figure 3 shows a more detailed view of a similar case with additional contour lines detailing the interior structure of the total ΔV in the region where there is relatively little change in total ΔV compared with the outer contour lines. A finer grid search and smaller changes in ΔV between contour lines are used in this interior region for the curved contours. Contour lines of 40.438, 40.439, 40.440, and 40.441 m/s are included, and all narrowly encompass the west and north sides of the invariant curve minima (with cost of 40.4379 m/s).

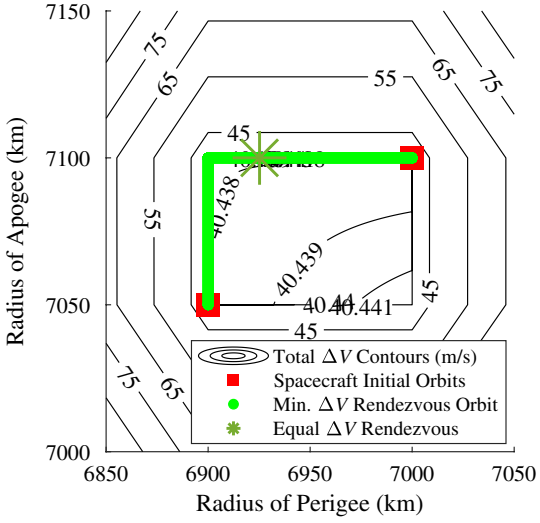

Fig. 3 ΔV optimal planar rendezvous orbits for a two-spacecraft system.

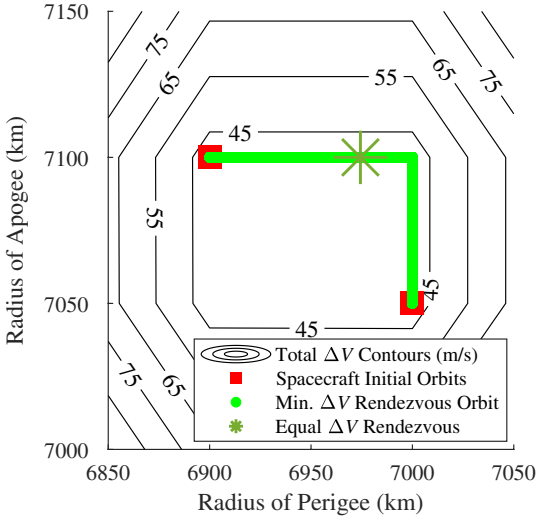

Fig. 4 ΔV optimal planar rendezvous orbits for a two-spacecraft system.

The invariant curve found here is the same result that was found in [15], which used the reachable set methodology of Holzinger et al. [6,22] to explore two-spacecraft rendezvous. Thus, the transfers used in this work appear to be consistent with the optimal transfer conditions used to calculate those reachable sets.

The point along the invariant curve where both spacecraft would expend the same amount of ΔV is also included. Because of the nonlinear relationships involved, the point of equal ΔV expenditure does not occur halfway along the invariant curve in ΔV space. To calculate the equal ΔV expenditure point a simple off-the-shelf root finding algorithm is used to search along the invariant curve.

B. Two-Spacecraft, Three-Dimensional Rendezvous

When the initial orbits of two spacecraft are not in the same plane, the previously observed invariant curve no longer exists. This result is expected, because the three-dimensional optimal transfers used here cannot equivalently be split into an infinite number of impulses. Instead, for two spacecraft in the three-dimensional case, two types of rendezvous solutions have been found. In the first type, there are two equivalent ΔV optimal rendezvous orbits, each coincident with the initial orbit of one of the spacecraft. That is, the minimum total ΔV rendezvous solution is for one of the spacecraft to transfer to the initial orbit of the other spacecraft. Figure 5 shows a sample scenario with two noncoplanar spacecraft where the minimum total ΔV rendezvous orbits are labeled as red dots. The partial derivatives of the total cost are discontinuous at each rendezvous solution, but are positive in each direction that the rendezvous orbit elements can be perturbed. That is,

$$\frac{\partial J_{\text{total}}}{\partial q_f^+} > 0 \qquad \frac{\partial J_{\text{total}}}{\partial q_f^-} > 0 \tag{19}$$

$$\frac{\partial J_{\text{total}}}{\partial Q_f^+} > 0 \qquad \frac{\partial J_{\text{total}}}{\partial Q_f^-} > 0 \tag{20}$$

$$\frac{\partial J_{\text{total}}}{\partial i_f^+} > 0 \qquad \frac{\partial J_{\text{total}}}{\partial i_f^-} > 0 \tag{21}$$

Although there are an infinite number of directions that the Gateaux (directional) derivative can be taken in this three-dimensional parameter space, each derivative can be approximated with a linear combination of these positive basis derivatives. Because each of these basis derivatives is positive, all Gateux derivatives must also be positive. This shows that these points satisfy the necessary and sufficient conditions for local minima. This has been confirmed with both analytic derivatives and finite differencing approximations of the partial derivatives of the cost.

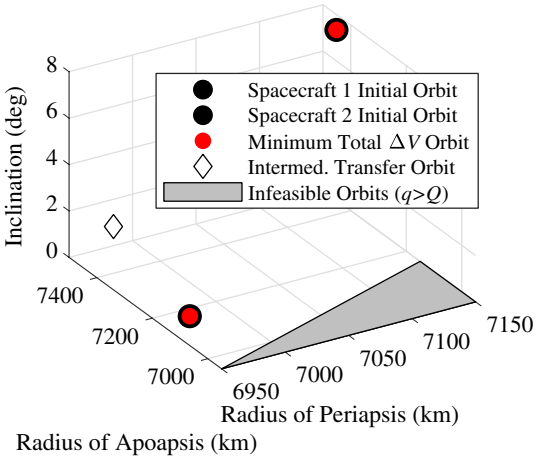

Fig. 5 Minimum total ΔV rendezvous orbits: two spacecraft, type 1.

To illustrate how a transfer would occur in Fig. 5, the intermediate transfer orbit has been included with a diamond marker. For either spacecraft to complete a transfer to the other spacecraft, it would first impulsively maneuver onto the transfer orbit and then impulsively maneuver to reach the initial orbit of the other spacecraft. In this case, $\eta = 0.2$ for the spacecraft with 0 inclination, and $\eta = 0.8$ for the spacecraft with an inclination of 7.4°. Thus, the transfer orbit has an inclination of 1.5°, which is 20% of the total inclination difference between the two spacecraft. Periapsis and apoapsis changes are made as in the planar case (see Fig. 1), but without the option of splitting changes to a single apsis into multiple impulses. Consequently, the transfer orbit has a periapsis radius equal to that of the 0 inclination spacecraft (6973 km) and apoapsis radius equal to that of the spacecraft with an inclination of 7.4° (7446 km).

The second type of two-spacecraft rendezvous orbit found is separate from the initial orbits of the two spacecraft. That is, in certain cases we find that either one or two total ΔV optimal rendezvous orbits are found in locations not coincident with the initial two spacecraft orbits. A simple example is shown in Fig. 6, where optimal rendezvous orbits for two noncoplanar spacecraft in circular orbits of equal radius are shown. In this case, it is actually advantageous for both spacecraft to rendezvous at one of two elliptical orbits of intermediate inclination where the periapsis radius is lower than the circular orbit radius and the apoapsis radius is larger than the circular orbit radius. In contrast to a pure plane change maneuver required for one spacecraft to match the initial orbit of the other, this rendezvous orbit allows the spacecraft to use more efficient plane changes at slower speeds, as well as the dogleg maneuver than can further minimize total ΔV. For both of the equivalent ΔV optimal rendezvous orbits in Fig. 6, both spacecraft would perform more than half of the total inclination change at apoapsis (i.e., $\eta < 0.5$, and in this case $\eta_1 = 0.18$ and $\eta_2 = 0.44$).

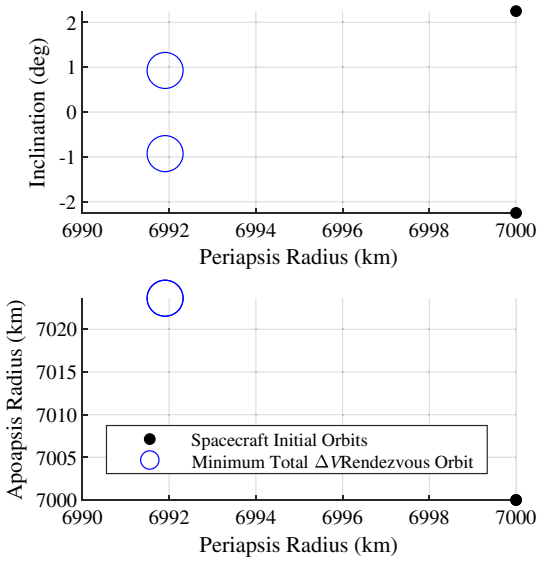

Fig. 6 Minimum total ΔV rendezvous orbits: two spacecraft, type 2.

Two equivalent optimal rendezvous orbits are found due to the symmetries of the two spacecraft initial orbits; they have equal and opposite inclinations as well as equal circular orbit altitudes. In test cases with this solution type but without such symmetries, single "separate" optimal rendezvous orbit are found. The ΔV cost improvement found in Fig. 6 is minor, however, at about 0.07% less total ΔV (0.4 m/s) than a simple transfer from one spacecraft initial orbit to the other's orbit. The ΔV savings found in other cases were also of similar magnitude. The magnitude of this cost improvement likely makes the discovery of these types of solutions more difficult. It is possible that this type of solution is always the true global optimum for the two spacecraft case, and the first type of coincident solution is only found due to a failure to find the noncoincident solution. In the case of Fig. 6 and other similar scenarios, a fine grid search combined with local gradient-based optimization with IPOPT [23] was used to find those solutions.

We can also demonstrate why the invariant curve does not exist for three-dimensional transfers by examining a scenario where suboptimal transfers are used to calculate the cost J_{total}. To calculate the suboptimal transfer, the cost J_{total} was calculated by assuming that the total inclination change was performed at the point in the Hohmann transfer where the spacecraft's speed was the lowest, giving a minimum of three impulses for the total transfer (2 maneuvers for the orbit shape changes, 1 maneuver for the inclination change). These suboptimal transfers allow the total transfer to be broken up into many impulses, so a type of invariant curve is again found, as seen in Fig. 7. In this case, there are a seemingly continuous number of options for final rendezvous orbits that cost the same total ΔV for both spacecraft, but with an inclination jump dividing the options. That is, all ΔV optimal rendezvous orbits share the same inclination as one of the spacecraft initial orbits.

C. More-Than-Two-Spacecraft, Planar Rendezvous

The grid search process can be extended to systems of more than 2 spacecraft. This results in total ΔV contour plots such as those in Figs. 8 (three spacecraft) and 9 (four spacecraft). The overall minimum ΔV orbit is now a single point, as opposed to the invariant curve observed for two-spacecraft systems. In Fig. 8a this minimum ΔV point happens to be coincident with the initial orbit of one of the spacecraft. But this is not always true, as seen in Fig. 8b. Also note that the minimum total ΔV rendezvous orbit does not lie on an intersection of all optimal transfer pathways between each pair of spacecraft in the system. The optimal transfer pathways between each pair of spacecraft are indicated with uniquely colored dotted lines in

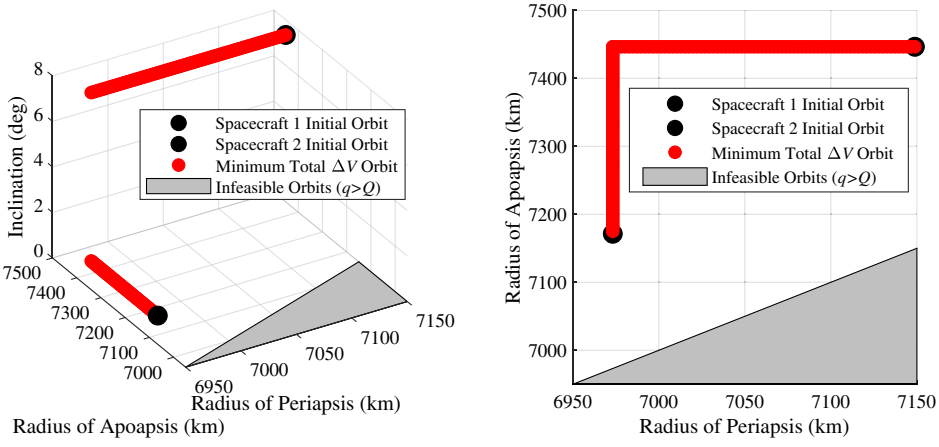

a) 3D view **b) 2D view**

Fig. 7 Minimum total ΔV rendezvous orbits without use of dogleg maneuvers.

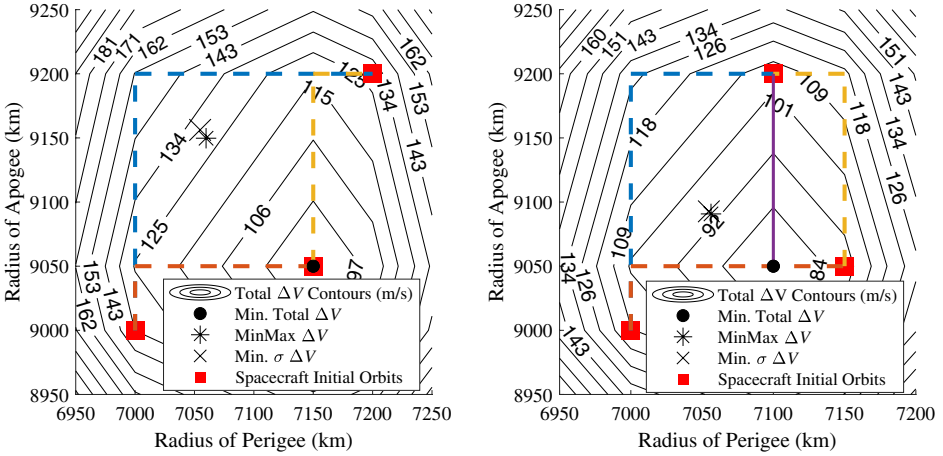

a) Scenario 1 b) Scenario 2

Fig. 8 Optimal rendezvous orbits for three-spacecraft systems. See Sec. IV.E for detail on MinMax ΔV and Min. $\sigma\Delta V$ orbits.

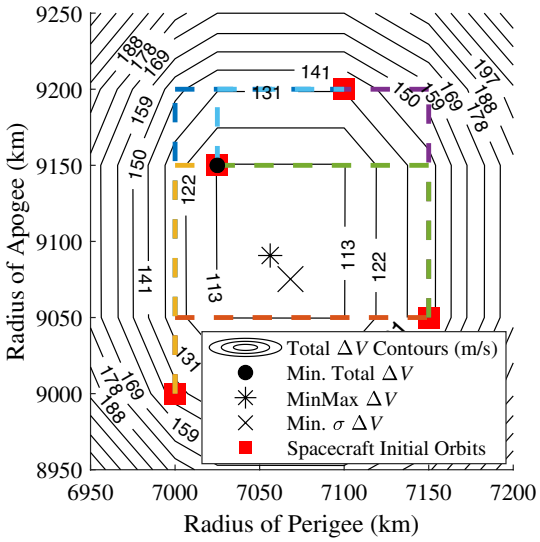

Fig. 9 Optimal rendezvous orbits for a four-spacecraft system.

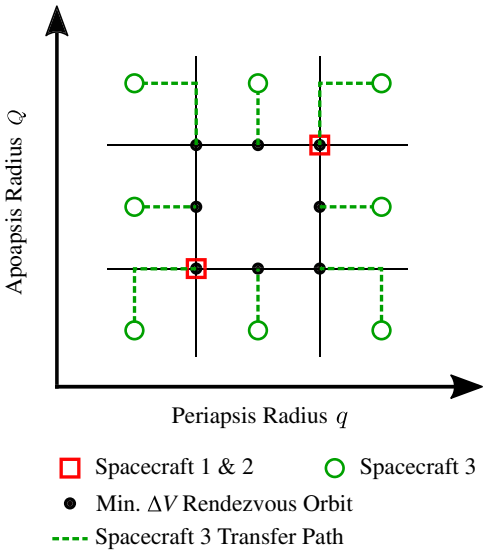

Fig. 10 Minimum ΔV rendezvous orbit location when adding third spacecraft.

Figs. 8, 9, 15, and 16. In Fig. 8b the optimal transfer path from the spacecraft with the largest Q to the minimum total ΔV rendezvous orbit is indicated with a purple solid line, because the rendezvous orbit does not lie on any of the interspacecraft transfer pathways connected to that spacecraft.

To explore the impact on the minimum ΔV rendezvous orbit when adding a third spacecraft to a two-spacecraft system, the orbit space is divided into nine sections as seen in Fig. 10. The grid is used to explore where the minimum total ΔV rendezvous orbit will lie if a third spacecraft is added to an existing system of two spacecraft in red. The interior box section defined by the two initial spacecraft is not considered, because if a third spacecraft were placed in that section, it could be considered one of the original two, with one of the other spacecraft being the third added spacecraft.

When a third spacecraft is added to the system, the minimum total ΔV rendezvous point will lie on the box whose corners are defined by the orbits of the initial two spacecraft. Further, the minimum total ΔV rendezvous orbit will be the point on the box that costs the least amount of ΔV for the third spacecraft to transfer to. The control policy shown in Fig. 1 also dictates the point on the box that will cost the least amount of ΔV. Although a static set of two spacecraft defines a box in Fig. 10, any two spacecraft for the three-spacecraft case can be selected to define the "box," and the minimum total ΔV rendezvous orbit will be located on the closest point on the box to the third spacecraft. With this in mind, the impact of adding a fourth spacecraft to a system of three spacecraft is considered.

In Fig. 11, there is a similar set of nine sections as in the three-spacecraft case in Fig. 10. Now, however, the interior section is the box defined by the initial three spacecraft, and the addition of a fourth spacecraft in different relative positions with respect to this interior box is explored. The locations of the minimum ΔV rendezvous orbit have some similarities to the three-spacecraft case, but two important differences. First, if a fourth spacecraft is added to the bottom middle section (at positions A or B), the minimum total ΔV rendezvous orbit lies within the box defined by the initial three spacecraft, as opposed to lying strictly on the box as in the three-spacecraft case. Second, although many minimum ΔV rendezvous orbits lie on the box defined by the three initial spacecraft, these points on the box are no longer strictly the closest point on the box to the orbit of the added spacecraft. For example, if a fourth spacecraft is added to the top left section at position C, the minimum total ΔV rendezvous orbit is not at the top left corner of the interior box as is the case in the three-spacecraft scenario. This implies that there is not a recursive relationship with respect to the location of minimum total ΔV orbit locations as more and more spacecraft are added to the system.

D. More-Than-Two-Spacecraft, Three-Dimensional Rendezvous

In the three-dimensional case with $N > 2$ where orbits exist in q–Q–i space, there are three types of solutions for minimum total ΔV rendezvous orbits that can be found. First, minimum ΔV orbits can be

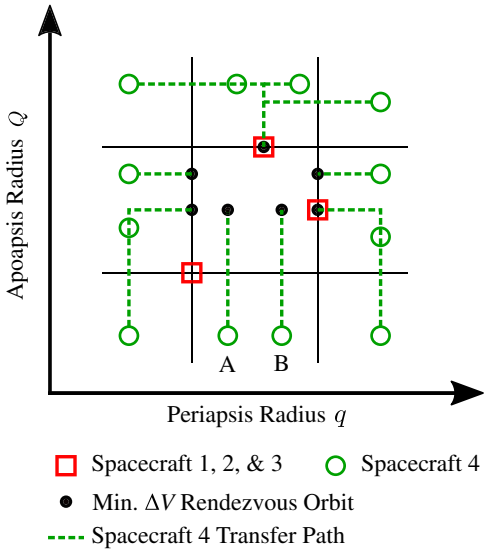

Fig. 11 Minimum ΔV rendezvous orbit location when adding fourth spacecraft.

found to be coincident with the initial orbit of one of the spacecraft, as seen in Fig. 12. In this case, it is ΔV optimal for all spacecraft to meet at the orbit of a single spacecraft. Like the two-spacecraft case, the partial derivatives of the cost function with respect to the rendezvous orbit elements are noncontinuous, but the cost is found to be increasing in each direction the orbit elements are varied.

Importantly, this is not the only type of minimum ΔV rendezvous orbit that is found. Some optimal orbits are also found to be interior to the initial conditions of the spacecraft. That is, the optimal rendezvous orbit lies within the range of initial spacecraft orbits, as in Fig. 13. In all test cases with interior solutions we found that the optimal rendezvous orbit shares at least one orbit element with one of the initial spacecraft orbits, but we cannot conclusively state that this is true in all cases of interior solutions. The interior region is perhaps the most natural range to search; one might expect that the optimal rendezvous orbit does not have a larger q, Q, or i than the highest spacecraft, or a smaller q, Q, or i than the lowest spacecraft. However, as seen in Fig. 14, sometimes the optimal rendezvous orbit will lie exterior to the range of spacecraft initial orbits. The optimal rendezvous orbit in Fig. 14 has a larger radius of apoapsis than any of the other spacecraft initial orbits. Solutions such as this one are in a region where the partial derivatives are continuous, so it is relatively simple to use an NLP solver to find the local minimum that satisfies the necessary conditions when starting from a more coarse approximation of the minimum provided by a grid search or evolutionary algorithm. Thus, when using this technique to optimize a given scenario, optimal solutions may be missed if a sufficiently large search space is not explored.

E. Alternative Optimization Criteria

The grid search method of finding total ΔV optimal rendezvous orbits also enables the use of alternative optimization criteria because the method involves calculating the ΔV cost for each individual spacecraft to transfer the rendezvous orbit. Of potential interest is minimizing the largest single ΔV expended by a spacecraft for a given rendezvous orbit. Figure 15 shows a contour plot of the

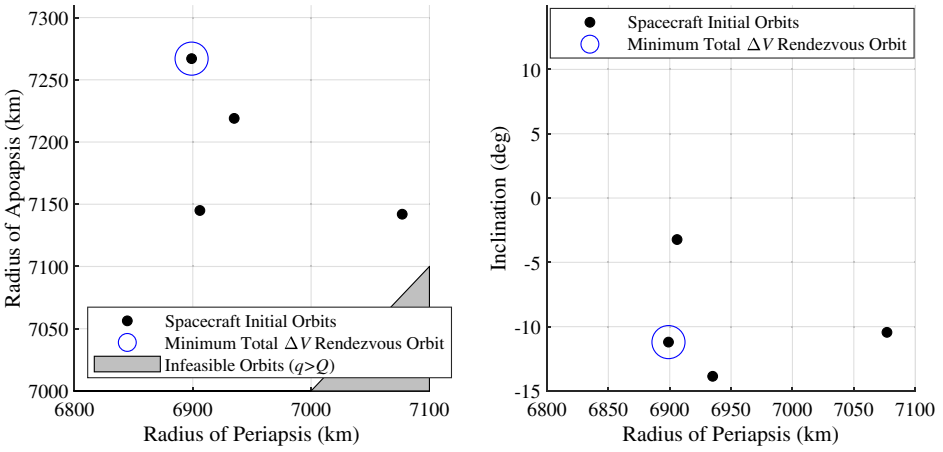

a) 2D View: Periapsis and Apoapsis **b) 2D View: Periapsis and Inclination**

Fig. 12 Minimum total ΔV rendezvous orbit coincident with initial spacecraft orbit.

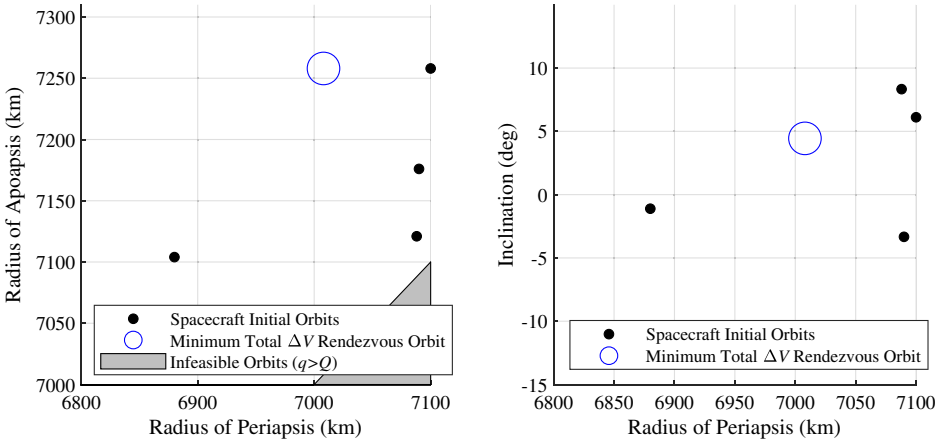

a) 2D View: Periapsis and Apoapsis **b) 2D View: Periapsis and Inclination**

Fig. 13 Minimum total ΔV rendezvous orbit interior to spacecraft initial conditions.

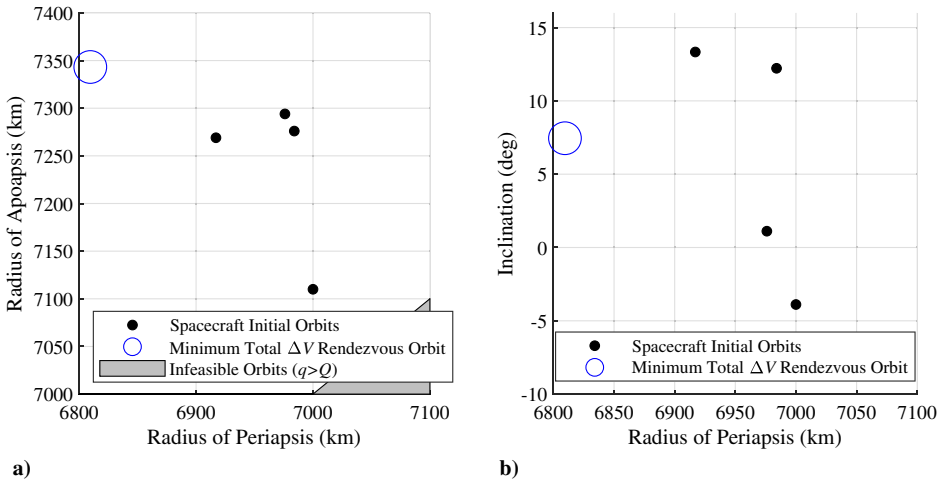

Fig. 14 Minimum total ΔV rendezvous orbit exterior to spacecraft initial conditions.

maximum single ΔV expended by a spacecraft for a planar, four-spacecraft system, with the smallest maximum indicated by a star.

Another criterion of interest is minimizing the standard deviation of the ΔV expended by each spacecraft to reach the rendezvous orbit. This is another method of preventing certain spacecraft from expending too much ΔV relative to its peers in a formation or swarm.

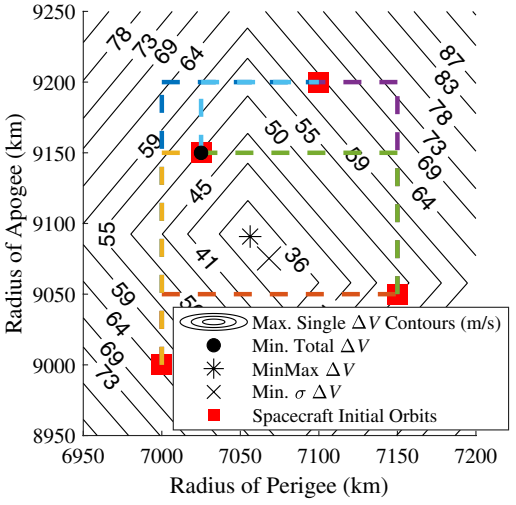

Fig. 15 Contour plot of maximum ΔV expended by a single spacecraft for each possible rendezvous orbit.

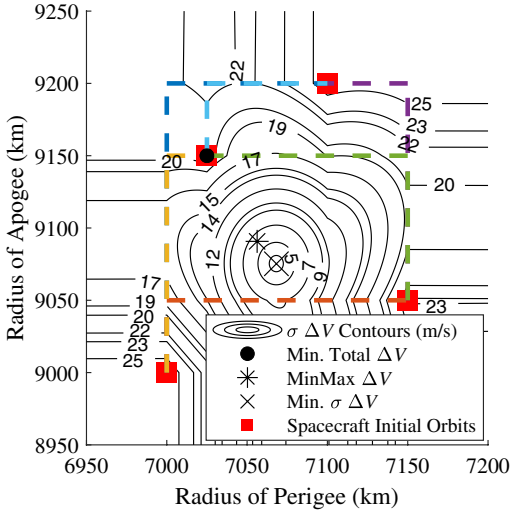

Fig. 16 Contour plot of the standard deviation of ΔV for all spacecraft.

Figure 16 shows contour plots of the standard deviation of all ΔV expenditures needed at each rendezvous orbit. Although the minimum σ orbit is close to the min/max point in both examples shown here, this is not always the case.

Note that these examples are planar for the purposes of visualization, but the same alternative optimization criteria can be applied in the three-dimensional case as well. The flexibility of this method further allows analysis of other cases, such as cases where a single spacecraft has limited fuel. Given the reachable set of a single limited spacecraft, options within that set can be explored with respect to the implications for the full formation.

V. Examples

A. Finite-Time Implementation for Full Rendezvous

Because the current method described thus far is time-free, it only describes a method of calculating optimal ΔV costs for a set of spacecraft to achieve the same q, Q, and i while J_2 perturbations and an indeterminate amount of time (possibly infinite) are used to allow the other three orbit elements to match for rendezvous. However, it is possible to realize in finite time these optimal ΔV costs that are found with the time-free method while using the same maneuvers found with that method. To demonstrate this, we begin with a set of N spacecraft with given initial values of $q_{0,k}$, $Q_{0,k}$, and $i_{0,k}$, where $k = 1, 2, \ldots, N$. Using the optimal rendezvous orbit a_f, e_f, and i_f found with the time-free method, we discuss how to find initial conditions for all spacecraft such that the time-free optimal ΔV cost is not exceeded for the spacecraft to further achieve the same argument of periapsis (ω_f), RAAN (Ω_f), and mean anomaly (M_f) at the rendezvous orbit in addition to achieving the same a_f, e_f, and i_f. Thus, we are investigating how to find $\Omega_{0,k}$, $\omega_{0,k}$, and $M_{0,k}$ at time t_0, and how to find ω_f, Ω_f, and $M_{0,f}$ of the rendezvous orbit such that the optimal ΔV value can be realized.

First, note that the optimal transfer sequence dictates that each of the two impulsive maneuvers for each spacecraft's transfer must be performed at periapsis or apoapsis. The spacecraft will also be restricted to an argument of periapsis $\omega_{i,k} = 0$ to ensure that maneuvers performed at periapsis or apoapsis also occur at an ascending or descending node. This is necessary given the velocity triangles used to find the equations for optimal ΔV costs; the velocity triangles used here assume that inclination changes occur at a node. Under these assumptions, no impulsive maneuver can change the orbit RAAN or ω, so these values need not be considered when targeting a set of final orbit elements. That is, $\omega_f = \omega_{i,k} = 0$, and $\Omega_{i,1} = \Omega_{i,2} = \ldots = \Omega_{i,N}$. This restricts all spacecraft to having the same initial RAAN, which will also be the same for the rendezvous orbit.

Further, the anomaly angle where the spacecraft inserts itself into the final orbit is dictated by the Hohmann transfer, and will occur at periapsis or apoapsis of the final orbit. Given these restrictions, a choice must be made as far as when each spacecraft should arrive at

the final rendezvous orbit. All spacecraft can only simultaneously arrive at the rendezvous orbit if the optimal transfer sequence dictates that they insert into the final orbit at the same true anomaly. This occurs when all spacecraft have a larger initial apoapsis radius than the rendezvous orbit (insert at rendezvous orbit periapsis) or if all spacecraft have a smaller initial apoapsis radius than the rendezvous orbit (insert at rendezvous orbit apoapsis). If neither is the case, then one set of spacecraft can insert at periapsis while the other inserts at apoapsis. Of course, this ignores operational concerns with having several spacecraft meet at the same point in space at the same time. Alternatively, each spacecraft can be assigned a unique time of periapsis or apoapsis passage on the rendezvous orbit for insertion.

As an example, we will find $M_{0,k}$ for all spacecraft in the scenario in Fig. 14, which has a rendezvous orbit with a larger apoapsis radius than all spacecraft in the system. In this case, all spacecraft maneuver first at their initial periapsis, and maneuver second at their final apoapsis. We will further assume that all spacecraft will meet at the same time at apoapsis of the final rendezvous orbit, though it will become apparent that the spacecraft initial conditions can be selected such that the spacecraft can insert into the rendezvous orbit at different apoapsis passage times.

The first step is to find the total transfer time from each spacecraft to the final rendezvous orbit. The subscript "tr" is used to indicate that a value corresponds to the transfer orbit being used to connect the initial and final orbits. The transfer time $t_{\mathrm{tr},k}$ is simply one half of the period of the transfer orbit connecting the initial and final orbits.

$$t_{\mathrm{tr},k} = \frac{T_{\mathrm{tr},k}}{2} = \pi\sqrt{\frac{a_{\mathrm{tr},k}^3}{\mu}}, \qquad k = 1, 2, \ldots, N \tag{22}$$

Further, a time of rendezvous t_f is set where the final rendezvous orbit has a mean anomaly $M_f = \pi$. Then, each spacecraft must have $M_{i,k} = 0$ at time $t_{i,k}$ when each spacecraft makes its first maneuver. With the given information, it is known that

$$t_{i,k} = t_f - t_{\mathrm{tr},k} \tag{23}$$

For spacecraft j that has the largest time $t_{\mathrm{tr},j}$, we set $t_f = t_{\mathrm{tr},j}$, so that $t_{i,j} = t_0 = 0$. We then simply need to use the times $t_{i,k}$ to find each $M_{0,k}$ from which after $t_{i,k}$ seconds $M_{i,k} = 0$.

If each spacecraft has an initial orbit mean motion of $n_{i,k}$, where

$$a_{i,k} = \frac{q_{i,k} + Q_{i,k}}{2} \tag{24}$$

$$n_{i,k} = \sqrt{\frac{\mu}{a_{i,k}^3}} \tag{25}$$

then

$$M_{0,k} = M_{i,k} - n_{i,k}t_{i,k} = -n_{i,k}t_{i,k} \tag{26}$$

The mean anomaly of the rendezvous orbit at time t_0, $M_{0,f}$, is

$$M_{0,f} = M_f - n_f t_f = \pi - n_f t_f \tag{27}$$

Thus, given the constants in Table 1, and for a system of four spacecraft with initial conditions listed in Table 2, we have found the remaining initial conditions shown in Table 3 that allow the spacecraft to rendezvous for the same ΔV cost found with the time-free ΔV optimal method. Note that initial and final ω and Ω have been set to 0 in this example; ω must be 0, but Ω can equivalently be any value that remains the same in the initial and rendezvous orbits.

This rendezvous scenario is illustrated in Fig. 17, where the transfer orbits are shown as solid lines, the final rendezvous orbit is shown with a black dotted line, and the initial spacecraft trajectories before the first maneuver are shown as colored dotted lines in Fig. 17b. Note that spacecraft 2 spends no time on its initial orbit, because in this simulation its first maneuver occurs at t_0. Figure 18 shows how q, Q, and i of each spacecraft varies over time. All spacecraft perform their final maneuver at the same time at the same rendezvous point in space, whereas the first maneuver time varies. The x-axis time scale of the Q plot is modified to show detail in the initial maneuver time; apoapsis remains unchanged after the first maneuver for each spacecraft.

The preceding method can be modified in a number of ways to adapt to different scenarios. For example, the spacecraft initial conditions can be found such that they insert into the rendezvous orbit at different times. This method can also be modified to work in scenarios where spacecraft must insert into different parts of the rendezvous orbit.

Finally, the secular orbit perturbation due to the J_2 term of a nonspherical central body can also be included. This perturbation secularly affects an orbit's Ω, ω, and the mean motion n. To account for these secular effects, the orbital period T in Eq. (22) should be replaced with

Table 2 Initial conditions for system of four spacecraft and the corresponding optimal rendezvous orbit

Value	Spacecraft 1	Spacecraft 2	Spacecraft 3	Spacecraft 4	Rendezvous
q_0, km	6984	7000	6976	6917	6809.5
Q_0, km	7276	7110	7294	7269	7343.2
i_0, deg	12.2	−3.9	1.1	13.3	7.452

Table 3 Remaining initial conditions to realize optimal rendezvous cost

Orbit	M, deg
Spacecraft 1 (M_0)	359.7
Spacecraft 2 (M_0)	0
Spacecraft 3 (M_0)	359.5
Spacecraft 4 (M_0)	358.4
Rendezvous orbit ($M_{0,f}$)	356.4

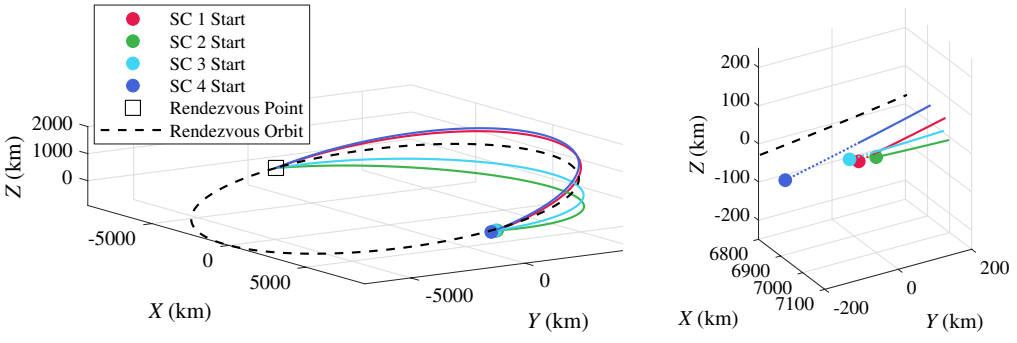

a) Wide View **b) Detail View of Start Points**

Fig. 17 Cartesian visualization of full rendezvous scenario.

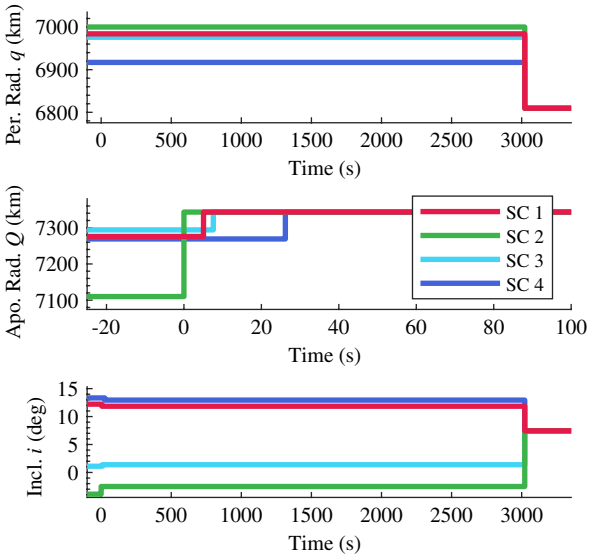

Fig. 18 Orbit elements over time for full rendezvous scenario.

$$\overline{T} = \frac{2\pi}{\overline{n}} \tag{28}$$

where $\overline{n}$ is the secular rate of mean anomaly given a J_2 perturbation. In Eqs. (26) and (27), $\overline{n}$ should also replace n, and it is given in [24] as

$$\overline{n} = n\left[1 + \frac{3C_{20}\sqrt{1-e^2}}{2p^2}\left(\frac{3}{2}\sin^2 i - 1\right)\right] \tag{29}$$

The secular rates of Ω and ω are also given in [24] as

$$\frac{d\overline{\omega}}{dt} = \frac{3nJ_2 r_c^2}{2p^2}\left(\frac{5}{2}\sin^2 i - 2\right) \tag{30}$$

$$\frac{d\overline{\Omega}}{dt} = \frac{3nJ_2 r_c^2}{2p^2}\cos i \tag{31}$$

where r_c is the radius of the central body. An important caveat here is that in the J_2 perturbed case, ω can no longer be held constant at 0 due to the secular drift $d\overline{\omega}/dt$. Thus, the maneuvers at periapsis and apoapsis will no longer occur at an ascending or descending node, and the velocity vector rotations in Fig. 2 [Eq. (13)] no longer directly translate to inclination changes. However, as a practical matter for Earth-orbiting spacecraft specifically, the secular drift rate $d\overline{\omega}/dt$ is on the order of 10^{-6} rad/s. Therefore, for practical, short-term considerations, ω can be considered to be essentially constant and can be set to be roughly 0.

Working backward from a certain desired rendezvous orbit Ω_f ($M_{0,f}$ is found in the same manner as before but with modified mean motion, ω is considered to be essentially constant), the changes in Ω as it is perturbed by J_2 throughout the transfer process must be accounted for. Because we take $\omega \approx 0$, and because each maneuver is only tangential at periapsis or apoapsis, each maneuver still will not impulsively change Ω, ω, or M. This can be observed, for example, by examining Gauss's variational equations [25]. Thus, to find the initial conditions $\Omega_{0,k}$, one can account for all changes in Ω with

$$\Omega_{0,k} = \Omega_f - t_{\mathrm{tr},k}\frac{d\overline{\Omega}}{dt} \tag{32}$$

Consequently, for the case where ω is set to be roughly 0, the optimal transfer results discussed here can be matched fairly closely in the J_2 perturbed case. The precession of Ω alone does not impact the theoretical ability to match the time- and orientation-free transfer cost. As ω deviates more from 0, the ΔV cost relative to these results will increase.

B. Constellation Deployment

One interesting application of this method is to find the optimal orbit from which to launch a constellation of several spacecraft. The deployment problem in this case is essentially rendezvous in reverse; the desired final orbits for spacecraft in the constellation can be fixed as the "initial conditions," and the minimum ΔV rendezvous orbit found in the same manner as above represents the optimal orbit from which to launch the spacecraft to their final orbits.

For a constellation of four spacecraft in circular, 7000 km orbits, with inclinations of −9°, −5.25°, 5.25°, and 9° (symmetric), the optimal deployment orbit is not actually a circular, 7000 km orbit. Rather, the optimal deployment orbit has 0° inclination, with $q =$ 6901 km and $Q = 7252$ km (exterior type solution). However, for a constellation of three spacecraft in circular, 7000 km orbits, with inclinations of −5.25°, 5.25°, and 0° (Fig. 19a), the optimal deployment orbit is a 7000 km circular orbit with 0° inclination (coincident-type solution). If two spacecraft of inclinations −9° and 9° are added to the previous case (Fig. 19b), the optimal deployment orbit shifts to $i = 0°$, $q = 7000$ km, and $Q = 7033$ km (exterior type solution). If the central spacecraft with final inclination of 0° in Fig. 19b is moved above or below 0° of inclination, the deployment orbit follows suit. For example, if the central spacecraft with inclination of 0° is moved to an inclination of 1°, the optimal deployment orbit will also have an inclination of 1°. This is generally found to be the case in "unbalanced" distributions; the ΔV optimal deployment orbit matches the inclination of the central spacecraft.

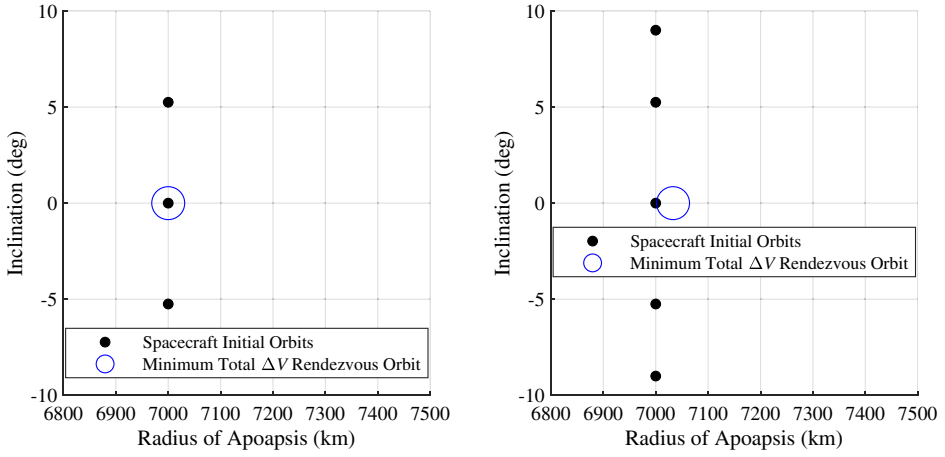

a) Three Spacecraft **b) Five Spacecraft**

Fig. 19 Optimal constellation deployment orbits.

Table 4 ΔV savings for different deployment scenarios

Final orbit inclinations, deg	ΔV cost savings over nominal deployment orbit, m/s	Optimal deployment orbit [q, Q, i], km, km, deg
[0, ±5.25, ±9]	2.7	[7000.0, 7033.1, 0]
[0, ±5.25, ±12]	8.4	[7000.0, 7064.6, 0]
[0, ±5.25, ±9, ±12]	26.9	[7000.0, 7148.8, 0]
[0, ±5.25, ±9, ±14]	37.9	[7000.0, 7184.9, 0]
[±5.25, ±9, ±12]	101.1	[6862.1, 7377.4, 0]
[±5.25, ±9, ±14]	126.1	[6853.4, 7445.5, 0]

The ΔV savings for the scenario in Fig. 19b are only about 2.7 m/s less total ΔV than if all spacecraft were to deploy from a nominal, circular deployment orbit with $q = 7000$, $Q = 7000$, and $i = 0$. However, as shown in Table 4, the cost savings over the nominal, circular deployment orbit grow as the destination orbits increase their final inclination values. The savings further increase if there is no spacecraft to be deployed at zero inclination. Also note that the optimal deployment orbits move farther and farther away from the 7000 km circular orbit as the ΔV savings increase.

This type of analysis can be useful when performing integrated systemwide optimization to determine what launch options, orbit planes, and satellite configurations are most cost-effective for a given set of constellation objectives. The notable result that some intermediate deployment orbit may provide relatively low total-ΔV-cost access to several different orbital inclinations may enable certain system architectures. The analysis here can be used as a starting point to explore the tradeoffs for which inclination orbits are best serviced by a single launcher, the amount of ΔV needed for each satellite to insert into its initial orbit, and the most economical number of satellites to place on a single launcher. Further, questions of ground coverage, overall satellite lifetime, and more can also be considered simultaneously along with those factors.

VI. Conclusions

Locations and lower bound costs of ΔV optimal cooperative rendezvous orbits for a system of many spacecraft can be found using time- and orientation-free ΔV optimal transfers. For two spacecraft in the same orbit plane, there are an infinite number of total ΔV optimal rendezvous orbits. As the number of spacecraft is increased and/or if the spacecraft are initially placed in different planes, the number of optimal rendezvous orbits is reduced to one. Importantly, the ΔV optimal rendezvous orbit is not necessarily at one of the initial orbits of one of the spacecraft. Although the methods used in the present work give lower bound ΔV costs for rendezvous where fuel is used only to change a, e, and i, it has also been shown that this lower bound cost for rendezvous is achievable in finite time with all spacecraft matching all orbit elements. Therefore, this lower bound is not overconservative and can be used in mission design scenarios or as a reference value.

Appendix: Partial Derivatives of the Optimal Orbit Transfer Cost

Partial derivatives of the analytic expression for the optimal orbit transfer cost in Eq. (13) can be useful for a number of different reasons, including for use with NLP solvers and for verifying that a solution is stationary. In this analysis initial orbit states are taken to be fixed, and changes in the cost function are explored with respect to changing final orbit parameters. Thus, the relevant partial derivatives to calculate are

$$\frac{\partial J}{\partial q_f} = \frac{\partial J}{\partial v_{1t}}\frac{\partial v_{1t}}{\partial q_f} + \frac{\partial J}{\partial \eta}\frac{\partial \eta}{\partial q_f} + \frac{\partial J}{\partial v_{2t}}\frac{\partial v_{2t}}{\partial q_f} + \frac{\partial J}{\partial v_f}\frac{\partial v_f}{\partial q_f} \tag{A1}$$

$$\frac{\partial J}{\partial Q_f} = \frac{\partial J}{\partial v_{1t}}\frac{\partial v_{1t}}{\partial Q_f} + \frac{\partial J}{\partial \eta}\frac{\partial \eta}{\partial Q_f} + \frac{\partial J}{\partial v_{2t}}\frac{\partial v_{2t}}{\partial Q_f} + \frac{\partial J}{\partial v_f}\frac{\partial v_f}{\partial Q_f} \tag{A2}$$

$$\frac{\partial J}{\partial i_f} = \frac{\partial J}{\partial \Delta i}\frac{\partial \Delta i}{\partial i_f} + \frac{\partial J}{\partial \eta}\frac{\partial \eta}{\partial i_f} \tag{A3}$$

In the multispacecraft rendezvous case, these partial derivatives are necessary for gradient-based parameter optimization algorithms, and help calculate necessary conditions for finding a minimum.

The following components of the partial derivatives are not dependent on the initial and final orbit values:

$$\frac{\partial J}{\partial v_{1t}} = \frac{1}{\Delta V_1}[v_{1t} - v_0\cos(\eta\Delta i)] \tag{A4}$$

$$\frac{\partial J}{\partial v_{2t}} = \frac{1}{\Delta V_2}[v_{2t} - v_f\cos((1-\eta)\Delta i)] \tag{A5}$$

$$\frac{\partial J}{\partial v_f} = \frac{1}{\Delta V_2}[v_f - v_{2t}\cos((1-\eta)\Delta i)] \tag{A6}$$

$$\frac{\partial J}{\partial \eta} = \frac{1}{\Delta V_1}[v_{1t}v_0\sin(\eta\Delta i)\Delta i] - \frac{1}{\Delta V_2}[v_f v_{2t}\sin((1-\eta)\Delta i)\Delta i] \tag{A7}$$

$$\frac{\partial J}{\partial \Delta i} = \frac{1}{\Delta V_1}[\eta v_{1t}v_0\sin(\eta\Delta i)] + \frac{1}{\Delta V_2}[(1-\eta)v_f v_{2t}\sin((1-\eta)\Delta i)] \tag{A8}$$

However, the partial derivatives of the velocities v_{1t}, v_{2t}, and v_f with respect to q_f and Q_f are dependent on the relative values of Q_f and Q_0. For $Q_f > Q_0$,

$$\frac{\partial v_{1t}}{\partial q_f} = 0 \tag{A9}$$

$$\frac{\partial v_{1t}}{\partial Q_f} = \frac{\mu}{v_{1t}(q_0+Q_f)^2} \tag{A10}$$

$$\frac{\partial v_{2t}}{\partial q_f} = 0 \tag{A11}$$

$$\frac{\partial v_{2t}}{\partial Q_f} = -\frac{\mu q_0(q_0+2Q_f)}{v_{2t}Q_f^2(q_0+Q_f)^2} \tag{A12}$$

$$\frac{\partial v_f}{\partial q_f} = \frac{\mu}{v_f(q_f+Q_f)^2} \tag{A13}$$

$$\frac{\partial v_f}{\partial Q_f} = -\frac{\mu q_f(q_f+2Q_f)}{v_f Q_f^2(q_f+Q_f)^2} \tag{A14}$$

For $Q_f \le Q_0$,

$$\frac{\partial v_{1t}}{\partial q_f} = \frac{\mu}{v_{1t}(q_f+Q_0)^2} \tag{A15}$$

$$\frac{\partial v_{1t}}{\partial Q_f} = 0 \tag{A16}$$

$$\frac{\partial v_{2t}}{\partial q_f} = -\frac{\mu Q_0(Q_0+2q_f)}{v_{2t}q_f^2(q_f+Q_0)^2} \tag{A17}$$

$$\frac{\partial v_{2t}}{\partial Q_f} = 0 \tag{A18}$$

$$\frac{\partial v_f}{\partial q_f} = -\frac{\mu Q_f(Q_f + 2q_f)}{v_f q_f^2 (q_f + Q_f)^2} \tag{A19}$$

$$\frac{\partial v_f}{\partial Q_f} = \frac{\mu}{v_f (q_f + Q_f)^2} \tag{A20}$$

Although there is no closed-form expression for η, partial derivatives of Eq. (15) can be used to solve for the needed partial derivatives of η. For example, the partial derivative of Eq. (15) with respect to q_f gives

$$\begin{aligned}\frac{\partial F}{\partial q_f} = &\frac{\partial F}{\partial v_{1t}}\frac{\partial v_{1t}}{\partial q_f} + \frac{\partial F}{\partial \Delta V_1}\left(\frac{\partial \Delta V_1}{\partial q_f} + \frac{\partial \Delta V_1}{\partial \eta}\frac{\partial \eta}{\partial q_f}\right) \\ &+ \frac{\partial F}{\partial v_{2t}}\frac{\partial v_{2t}}{\partial q_f} + \frac{\partial F}{\partial v_f}\frac{\partial v_f}{\partial q_f} + \frac{\partial F}{\partial \Delta V_2}\left(\frac{\partial \Delta V_2}{\partial q_f} + \frac{\partial \Delta V_2}{\partial \eta}\frac{\partial \eta}{\partial q_f}\right) \\ &+ \frac{\partial F}{\partial \eta}\frac{\partial \eta}{\partial q_f} = 0\end{aligned} \tag{A21}$$

which can be solved for $\partial\eta/\partial q_f$, giving the result

$$\begin{aligned}\frac{\partial \eta}{\partial q_f} = -&\left[\frac{\partial F}{\partial v_{1t}}\frac{\partial v_{1t}}{\partial q_f} + \frac{\partial F}{\partial \Delta V_1}\frac{\partial \Delta V_1}{\partial q_f} + \frac{\partial F}{\partial v_{2t}}\frac{\partial v_{2t}}{\partial q_f} + \frac{\partial F}{\partial v_f}\frac{\partial v_f}{\partial q_f} + \frac{\partial F}{\partial \Delta V_2}\frac{\partial \Delta V_2}{\partial q_f}\right] \\ &\Big/\left[\frac{\partial F}{\partial \eta} + \frac{\partial F}{\partial \Delta V_2}\frac{\partial \Delta V_2}{\partial \eta} + \frac{\partial F}{\partial \Delta V_1}\frac{\partial \Delta V_1}{\partial \eta}\right]\end{aligned} \tag{A22}$$

Similarly, solving for $\partial\eta/\partial Q_f$ gives

$$\begin{aligned}\frac{\partial \eta}{\partial Q_f} = -&\left[\frac{\partial F}{\partial v_{1t}}\frac{\partial v_{1t}}{\partial Q_f} + \frac{\partial F}{\partial \Delta V_1}\frac{\partial \Delta V_1}{\partial Q_f} + \frac{\partial F}{\partial v_{2t}}\frac{\partial v_{2t}}{\partial Q_f} + \frac{\partial F}{\partial v_f}\frac{\partial v_f}{\partial Q_f} + \frac{\partial F}{\partial \Delta V_2}\frac{\partial \Delta V_2}{\partial Q_f}\right] \\ &\Big/\left[\frac{\partial F}{\partial \eta} + \frac{\partial F}{\partial \Delta V_2}\frac{\partial \Delta V_2}{\partial \eta} + \frac{\partial F}{\partial \Delta V_1}\frac{\partial \Delta V_1}{\partial \eta}\right]\end{aligned} \tag{A23}$$

Finally, solving for $\partial\eta/\partial i_f$ gives

$$\begin{aligned}\frac{\partial \eta}{\partial i_f} = -&\left[\frac{\partial F}{\partial \Delta i}\frac{\partial \Delta i}{\partial i_f} + \frac{\partial F}{\partial \Delta V_1}\frac{\partial \Delta V_1}{\partial \Delta i}\frac{\partial \Delta i}{\partial i_f} + \frac{\partial F}{\partial \Delta V_2}\frac{\partial \Delta V_2}{\partial \Delta i}\frac{\partial \Delta i}{\partial i_f}\right] \\ &\Big/\left[\frac{\partial F}{\partial \eta} + \frac{\partial F}{\partial \Delta V_2}\frac{\partial \Delta V_2}{\partial \eta} + \frac{\partial F}{\partial \Delta V_1}\frac{\partial \Delta V_1}{\partial \eta}\right]\end{aligned} \tag{A24}$$

The following additional partial derivatives are needed to evaluate Eqs. (A22–A24).

$$\frac{\partial \Delta i}{\partial i_f} = \begin{cases} 1 & i_f > i_0 \\ -1 & i_f < i_0 \end{cases} \tag{A25}$$

$$\frac{\partial \Delta V_1}{\partial q_f} = \frac{1}{\Delta V_1}\left[v_{1t}\frac{\partial v_{1t}}{\partial q_f} - v_0 \cos(\eta \Delta i)\frac{\partial v_{1t}}{\partial q_f}\right] \tag{A26}$$

$$\frac{\partial \Delta V_1}{\partial Q_f} = \frac{1}{\Delta V_1}\left[v_{1t}\frac{\partial v_{1t}}{\partial Q_f} - v_0 \cos(\eta \Delta i)\frac{\partial v_{1t}}{\partial Q_f}\right] \tag{A27}$$

$$\begin{aligned}\frac{\partial \Delta V_2}{\partial q_f} = &\frac{1}{\Delta V_2}\left[v_f\frac{\partial v_f}{\partial q_f} + v_{2t}\frac{\partial v_{2t}}{\partial q_f}\right. \\ &\left. - \left(v_{2t}\cos((1-\eta)\Delta i)\frac{\partial v_f}{\partial q_f} + v_f \cos((1-\eta)\Delta i)\frac{\partial v_{2t}}{\partial q_f}\right)\right]\end{aligned} \tag{A28}$$

$$\begin{aligned}\frac{\partial \Delta V_2}{\partial Q_f} = &\frac{1}{\Delta V_2}\left[v_f\frac{\partial v_f}{\partial Q_f} + v_{2t}\frac{\partial v_{2t}}{\partial Q_f}\right. \\ &\left. - \left(v_{2t}\cos((1-\eta)\Delta i)\frac{\partial v_f}{\partial Q_f} + v_f \cos((1-\eta)\Delta i)\frac{\partial v_{2t}}{\partial Q_f}\right)\right]\end{aligned} \tag{A29}$$

$$\frac{\partial \Delta V_1}{\partial \eta} = \frac{v_{1t} v_0 \sin(\eta \Delta i)\Delta i}{\Delta V_1} \tag{A30}$$

$$\frac{\partial \Delta V_2}{\partial \eta} = \frac{-v_{2t} v_f \sin((1-\eta)\Delta i)\Delta i}{\Delta V_2} \tag{A31}$$

$$\frac{\partial F}{\partial v_{1t}} = \frac{\Delta i v_0 \sin(\eta \Delta i)}{\Delta V_1} \tag{A32}$$

$$\frac{\partial F}{\partial v_{2t}} = \frac{-\Delta i v_f \sin((1-\eta)\Delta i)}{\Delta V_2} \tag{A33}$$

$$\frac{\partial F}{\partial v_f} = \frac{-\Delta i v_{2t} \sin((1-\eta)\Delta i)}{\Delta V_2} \tag{A34}$$

$$\frac{\partial F}{\partial \Delta V_1} = \frac{-\Delta i v_0 v_{1t} \sin(\eta \Delta i)}{\Delta V_1^2} \tag{A35}$$

$$\frac{\partial F}{\partial \Delta V_2} = \frac{\Delta i v_f v_{2t} \sin((1-\eta)\Delta i)}{\Delta V_2^2} \tag{A36}$$

$$\begin{aligned}\frac{\partial F}{\partial \eta} = &\frac{\Delta i^2 v_0 v_{1t} \cos(\eta \Delta i)}{\Delta V_1} - \frac{\Delta i v_0 v_{1t} \sin(\eta \Delta i)}{\Delta V_1^2}\frac{\partial \Delta V_1}{\partial \eta} \\ &+ \ldots \frac{\Delta i^2 v_f v_{2t} \cos((1-\eta)\Delta i)}{\Delta V_2} + \frac{\Delta i v_f v_{2t} \sin((1-\eta)\Delta i)}{\Delta V_2^2}\frac{\partial \Delta V_2}{\partial \eta}\end{aligned} \tag{A37}$$

$$\begin{aligned}\frac{\partial F}{\partial \Delta i} = &\frac{v_0 v_{1t}[\sin(\eta \Delta i) + \eta \Delta i \cos(\eta \Delta i)]}{\Delta V 1} - \frac{\Delta i v_0 v_{1t} \sin(\eta \Delta i)}{\Delta V_1^2}\frac{\partial \Delta V_1}{\partial \Delta i} \\ &- \ldots \frac{v_f v_{2t}[\sin((1-\eta)\Delta i) - \eta \Delta i \cos((1-\eta)\Delta i)]}{\Delta V_2} \\ &+ \frac{\Delta i v_f v_{2t} \sin((1-\eta)\Delta i)}{\Delta V_2^2}\frac{\partial \Delta V_2}{\partial \Delta i}\end{aligned} \tag{A38}$$

Importantly, the derivatives presented here are only continuous in certain regions of state space. These regions are bounded by planes where one of the orbit elements q_f, Q_f, or i_f are equal to one of the initial orbit elements of the active spacecraft $q_{0,j}$, $Q_{0,j}$, or $i_{0,j}$, respectively.

1. $q_0 = q_f$, $Q_0 = Q_f$, and $i_0 = i_f$

In the case where $q_0 = q_f$, $Q_0 = Q_f$, and $i_0 = i_f$, the nominal impulsive ΔV magnitudes are zero, and the above expressions break down. However, nominal ΔV cost equations can be rewritten based on the parameter to be varied. For example, to change i_f only, the optimal maneuver ΔV cost is

$$\Delta V = 2V_Q \sin\left(\frac{\Delta i}{2}\right) \approx V_Q \Delta i \tag{A39}$$

for small ΔV and

$$V_Q = \sqrt{2\mu \frac{q}{Q(q+Q)}} \tag{A40}$$

is the speed at apoapsis. Thus,

$$\frac{\partial \Delta V}{\partial i_f} = \begin{cases} V_Q & i_f > i_0 \\ -V_Q & i_f < i_0 \end{cases} \tag{A41}$$

Considering an impulsive maneuver to change just q_f, the ΔV cost is

$$\Delta V = \begin{cases} v_f - v_0 & q_f > q_0 \\ v_0 - v_f & q_f < q_0 \end{cases} \tag{A42}$$

where

$$v_0 = \sqrt{2\mu \frac{q_0}{Q(q_0 + Q)}} \tag{A43}$$

$$v_f = \sqrt{2\mu \frac{q_f}{Q(q_f + Q)}} \tag{A44}$$

This gives the result

$$\frac{\partial \Delta V}{\partial q_f} = \begin{cases} \dfrac{\partial v_f}{\partial q_f} & q_f > q_0 \\ -\dfrac{\partial v_f}{\partial q_f} & q_f < q_0 \end{cases} \tag{A45}$$

with

$$\frac{\partial v_f}{\partial q_f} = \frac{\mu}{v_f (q_f + Q)^2} \tag{A46}$$

Finally, considering an impulsive maneuver to change just Q_f, the ΔV cost is

$$\Delta V = \begin{cases} v_f - v_0 & Q_f > Q_0 \\ v_0 - v_f & Q_f < Q_0 \end{cases} \tag{A47}$$

where

$$v_0 = \sqrt{2\mu \frac{Q_0}{q(q + Q_0)}} \tag{A48}$$

$$v_f = \sqrt{2\mu \frac{Q_f}{q(q + Q_f)}} \tag{A49}$$

This gives the result

$$\frac{\partial \Delta V}{\partial Q_f} = \begin{cases} \dfrac{\partial v_f}{\partial Q_f} & Q_f > Q_0 \\ -\dfrac{\partial v_f}{\partial Q_f} & Q_f < Q_0 \end{cases} \tag{A50}$$

with

$$\frac{\partial v_f}{\partial Q_f} = \frac{\mu}{v_f (q + Q_f)^2} \tag{A51}$$

Acknowledgments

This work was supported by a NASA Space Technology Research Fellowship. Portions of this work were presented as Paper IAC-18-C1.5.2 at the 2018 International Astronautical Congress, Bremen, Germany, October 1–5, 2018.

References

[1] Scharf, D. P., Hadaegh, F. Y., and Ploen, S. R., "A Survey of Spacecraft Formation Flying Guidance and Control (Part 1): Guidance," *Proceedings of the 2003 American Control Conference*, Vol. 2, Inst. of Electrical and Electronics Engineers, New York, 2003, pp. 1733–1739. https://doi.org/10.1109/ACC.2003.1239845

[2] Scharf, D. P., Hadaegh, F. Y., and Ploen, S. R., "A Survey of Spacecraft Formation Flying Guidance and Control. Part II: Control," *Proceedings of the 2004 American Control Conference*, Vol. 4, Inst. of Electrical and Electronics Engineers, New York, 2004, pp. 2976–2985. https://doi.org/10.23919/ACC.2004.1384365

[3] Alfriend, K., Vadali, S. R., Gurfil, P., How, J., and Breger, L., *Spacecraft Formation Flying: Dynamics, Control and Navigation*, Butterworth-Heinemann, Oxford, 2009, Chap. 10. https://doi.org/10.1016/C2009-0-17485-8

[4] Gobetz, F. W., and Doll, J. R., "A Survey of Impulsive Trajectories," *AIAA Journal*, Vol. 7, No. 5, 1969, pp. 801–834. https://doi.org/10.2514/3.5231

[5] Hohmann, W., "The Attainability of Heavenly Bodies (Die Ereichbarkeit der Himrnelskorper)," NASA Technical Translations F-44, 1960.

[6] Holzinger, M. J., Scheeres, D. J., and Erwin, R. S., "On-Orbit Operational Range Computation Using Gauss's Variational Equations with J2 Perturbations," *Journal of Guidance, Control, and Dynamics*, Vol. 37, No. 2, 2014, pp. 608–622. https://doi.org/10.2514/1.53861

[7] Prussing, J. E., *Optimal Spacecraft Trajectories*, Oxford Univ. Press, Oxford, 2017, Chap. 7. https://doi.org/10.1093/oso/9780198811084.001.0001

[8] Prussing, J., "Terminal Maneuver for an Optimal Cooperative Impulsive Rendezvous (AAS 97-649)," *Advances in the Astronautical Sciences*, Vol. 97, Part I, 1998, pp. 759–772.

[9] Prussing, J. E., and Conway, B. A., "Optimal Terminal Maneuver for a Cooperative Impulsive Rendezvous," *Journal of Guidance, Control, and Dynamics*, Vol. 12, No. 3, 1989, pp. 433–435. https://doi.org/10.2514/3.20427

[10] Coverstone-Carroll, V., and Prussing, J. E., "Optimal Cooperative Power-Limited Rendezvous Between Neighboring Circular Orbits," *Journal of Guidance, Control, and Dynamics*, Vol. 16, No. 6, 1993, pp. 1045–1054. https://doi.org/10.2514/3.21126

[11] Coverstone-Carroll, V., and Prussing, J. E., "Optimal Cooperative Power-Limited Rendezvous Between Coplanar Circular Orbits," *Journal of Guidance, Control, and Dynamics*, Vol. 17, No. 5, 1994, pp. 1096–1102. https://doi.org/10.2514/3.21315

[12] Dutta, A., and Tsiotras, P., "Hohmann-Hohmann and Hohmann-Phasing Cooperative Rendezvous Maneuvers," *Journal of the Astronautical Sciences*, Vol. 57, No. 1, 2009, pp. 393–417. https://doi.org/10.1007/BF03321510

[13] Bevilacqua, R., and Romano, M., "Rendezvous Maneuvers of Multiple Spacecraft Using Differential Drag Under J2 Perturbation," *Journal of Guidance, Control, and Dynamics*, Vol. 31, No. 6, 2008, pp. 1595–1607. https://doi.org/10.2514/1.36362

[14] Thakur, D., Hernandez, S., and Akella, M. R., "Spacecraft Swarm Finite-Thrust Cooperative Control for Common Orbit Convergence," *Journal of Guidance, Control, and Dynamics*, Vol. 38, No. 3, 2015, pp. 478–488. https://doi.org/10.2514/1.G000621

[15] Venigalla, C., and Scheeres, D., "Spacecraft Rendezvous and Pursuit/Evasion Analysis Using Reachable Sets," *28th AAS/AIAA Space Flight Mechanics Meeting*, AIAA Paper 2018-0219, 2018. https://doi.org/10.2514/6.2018-0219

[16] Broucke, R. A., and Prado, A. F. B. A., "Orbital Planar Maneuvers Using Two and Three-Four (Through Infinity) Impulses," *Journal of Guidance, Control, and Dynamics*, Vol. 19, No. 2, 1996, pp. 274–282. https://doi.org/10.2514/3.21615

[17] Mease, K. D., and Rao, A. V., *Minimum-Fuel Transfer Between Coplanar Elliptic Orbits—Global Results Using Green's Theorem*, Springer, Berlin, 1994, pp. 113–125. https://doi.org/10.1007/978-1-4615-2425-0_12

[18] Chobotov, V. A., *Orbital Mechanics*, 3rd ed., AIAA, Reston, VA, 2002, Chap. 5. https://doi.org/10.2514/4.862250

[19] Rider, L., "Characteristic Velocity Requirements for Impulsive Thrust Transfers Between Non Co-Planar Circular Orbits," *ARS Journal*, Vol. 31, No. 3, 1961, pp. 345–351. https://doi.org/10.2514/8.5478

[20] Anthony, M., and Fosdick, G., "Optimum Two-Impulse, Conodal Transfers Between Inclined Circular Orbits," *Proceedings of the Fifth International Symposium on Space Technology and Science*, 1964, p. 443.

[21] Drezner, Z., and Hamacher, H. W., *Facility Location: Applications and Theory*, Springer Science & Business Media, Berlin, 2001, p. 2.
[22] Holzinger, M. J., Scheeres, D. J., and Hauser, J., "Reachability Using Arbitrary Performance Indices," *IEEE Transactions on Automatic Control*, Vol. 60, No. 4, 2015, pp. 1099–1103. https://doi.org/10.1109/TAC.2015.2391451
[23] Wächter, A., and Biegler, L. T., "On the Implementation of an Interior-Point Filter Line-Search Algorithm for Large-Scale Nonlinear Programming," *Mathematical Programming*, Vol. 106, No. 1, 2006, pp. 25–57. https://doi.org/10.1007/s10107-004-0559-y
[24] Scheeres, D. J., *Orbital Motion in Strongly Perturbed Environments: Applications to Asteroid, Comet and Planetary Satellite Orbiters*, Springer, Berlin, 2012, p. 178. https://doi.org/10.1007/978-3-642-03256-1
[25] Schaub, H., and Junkins, J. L., *Analytical Mechanics of Space Systems*, AIAA, Reston, VA, 2005, Chap. 12. https://doi.org/10.2514/4.105210